

NUCLEAR DATA AND MEASUREMENTS SERIES

ANL/NDM-86

**Energy-Differential Cross Section Measurement
for the $^{51}\text{V}(\text{n},\alpha)^{48}\text{Sc}$ Reaction**

by

Ikuo Kanno, James W. Meadows, and Donald L. Smith

July 1984

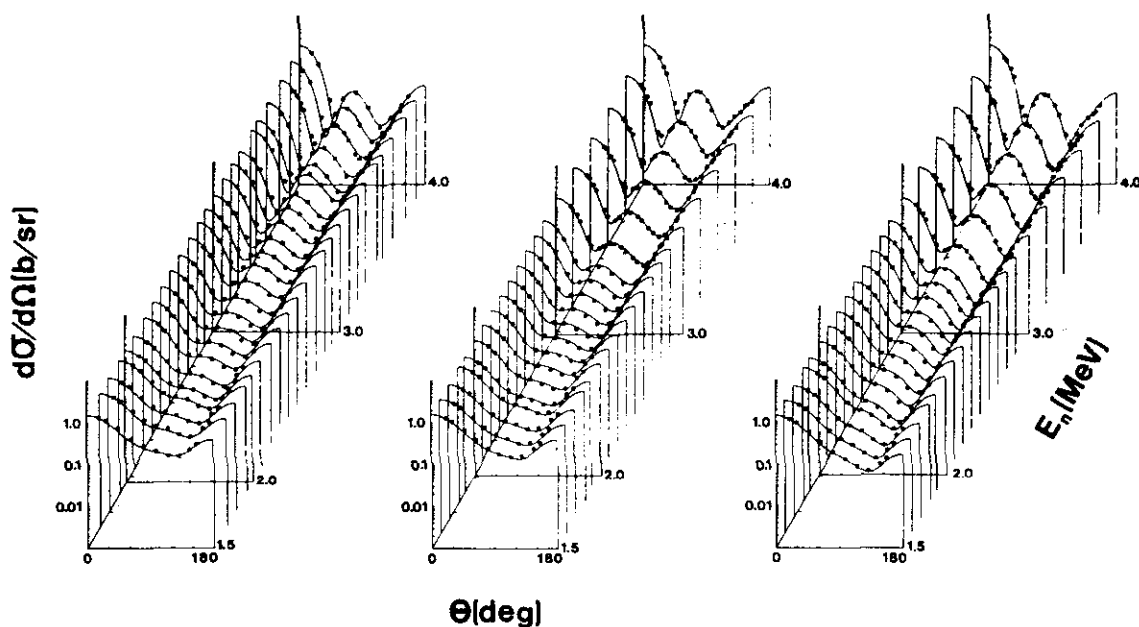
**ARGONNE NATIONAL LABORATORY,
ARGONNE, ILLINOIS 60439, U.S.A.**

NUCLEAR DATA AND MEASUREMENTS SERIES

ANL/NDM-86
ENERGY-DIFFERENTIAL CROSS SECTION MEASUREMENT FOR THE
 $^{51}\text{V}(n,\alpha)^{48}\text{Sc}$ REACTION*

by
Ikuo Kanno**, James W. Meadows and Donald L. Smith

July 1984



ARGONNE NATIONAL LABORATORY, ARGONNE, ILLINOIS

Operated by THE UNIVERSITY OF CHICAGO

for the U. S. DEPARTMENT OF ENERGY

under Contract W-31-109-Eng-38

Argonne National Laboratory, with facilities in the states of Illinois and Idaho, is owned by the United States government, and operated by The University of Chicago under the provisions of a contract with the Department of Energy.

DISCLAIMER

This report was prepared as an account of work sponsored by an agency of the United States Government. Neither the United States Government nor any agency thereof, nor any of their employees, makes any warranty, express or implied, or assumes any legal liability or responsibility for the accuracy, completeness, or usefulness of any information, apparatus, product, or process disclosed, or represents that its use would not infringe privately owned rights. Reference herein to any specific commercial product, process, or service by trade name, trademark, manufacturer, or otherwise, does not necessarily constitute or imply its endorsement, recommendation, or favoring by the United States Government or any agency thereof. The views and opinions of authors expressed herein do not necessarily state or reflect those of the United States Government or any agency thereof.

ANL/NDM-86
ENERGY-DIFFERENTIAL CROSS SECTION MEASUREMENT FOR THE
 $^{51}\text{V}(n,\alpha)^{48}\text{Sc}$ REACTION*

by

Ikuo Kanno**, James W. Meadows and Donald L. Smith

July 1984

E

NUCLEAR REACTION $^{51}\text{V}(n,\alpha)^{48}\text{Sc}$. Measured $\sigma_{n\alpha}(E_n)$ $E_n =$
5.515 - 9.567 MeV. Activation method. Counted 0.984-, 1.037-
and 1.312- MeV ^{48}Sc -decay gamma rays. Measured ^{48}Sc half life.
Standard: ENDF/B-V $\sigma_f(E_n)$ for ^{238}U . Detailed uncertainty
analysis. Integral-differential comparisons for ^{235}U and ^{252}Cf
fission-neutron spectra.

Applied Physics Division
Argonne National Laboratory
9700 South Cass Avenue
Argonne, Illinois 60439
USA

*This work supported by the U.S. Department of Energy.

**Exchange Associate. Permanent Address: Research Reactor Institute,
Kyoto University, Kumatori-Cho, Sennan-Gun, Osaka 590-04, Japan.

NUCLEAR DATA AND MEASUREMENTS SERIES

The Nuclear Data and Measurements Series presents results of studies in the field of microscopic nuclear data. The primary objective is the dissemination of information in the comprehensive form required for nuclear technology applications. This Series is devoted to: a) measured microscopic nuclear parameters, b) experimental techniques and facilities employed in measurements, c) the analysis, correlation and interpretation of nuclear data, and d) the evaluation of nuclear data. Contributions to this Series are reviewed to assure technical competence and, unless otherwise stated, the contents can be formally referenced. This Series does not supplant formal journal publication but it does provide the more extensive information required for technological applications (e.g., tabulated numerical data) in a timely manner.

INFORMATION ABOUT OTHER ISSUES IN THE ANL/NDM SERIES:

A list of titles and authors for reports ANL/NDM-1 through ANL/NDM-50 can be obtained by referring to any report of this series numbered ANL/NDM-51 through ANL/NDM-76. Requests for a complete list of titles or for copies of previous reports should be directed to:

Section Secretary
Applied Nuclear Physics Section
Applied Physics Division
Building 316
Argonne National Laboratory
9700 South Cass Avenue
Argonne, Illinois 60439
USA

- ANL/NDM-51 Measured and Evaluated Neutron Cross Sections of Elemental Bismuth by A. Smith, P. Guenther, D. Smith and J. Whalen, April 1980.
- ANL/NDM-52 Neutron Total and Scattering Cross Sections of ${}^6\text{Li}$ in the Few MeV Region by P. Guenther, A. Smith and J. Whalen, February 1980.
- ANL/NDM-53 Neutron Source Investigations in Support of the Cross Section Program at the Argonne Fast-Neutron Generator by James W. Meadows and Donald L. Smith, May 1980.
- ANL/NDM-54 The Nonelastic-Scattering Cross Sections of Elemental Nickel by A. B. Smith, P. T. Guenther and J. F. Whalen, June 1980.
- ANL/NDM-55 Thermal Neutron Calibration of a Tritium Extraction Facility using the ${}^6\text{Li}(n,t){}^4\text{He}/{}^{197}\text{Au}(n,\gamma){}^{198}\text{Au}$ Cross Section Ratio for Standardization by M. M. Bretscher and D. L. Smith, August 1980.
- ANL/NDM-56 Fast-Neutron Interactions with ${}^{182}\text{W}$, ${}^{184}\text{W}$ and ${}^{186}\text{W}$ by P. T. Guenther, A. B. Smith and J. F. Whalen, December 1980.
- ANL/NDM-57 The Total, Elastic- and Inelastic-Scattering Fast-Neutron Cross Sections of Natural Chromium by Peter T. Guenther, Alan B. Smith and James F. Whalen, January 1981.
- ANL/NDM-58 Review of Measurement Techniques for the Neutron Capture Process by W. P. Poenitz, August 1981.
- ANL/NDM-59 Review of the Importance of the Neutron Capture Process in Fission Reactors by Wolfgang P. Poenitz, July 1981.
- ANL/NDM-60 Gamma-Ray Detector Calibration Methods Utilized in the Argonne FNG Group Activation Cross Section Measurement Program by James W. Meadows and Donald L. Smith, April 1984 [Present report-see notice at the end of this list].

- ANL/NDM-61 Fast-neutron Total and Scattering Cross Sections of ^{58}Ni by Carl Budtz-Jørgensen, Peter T. Guenther, Alan B. Smith and James F. Whalen, September 1981.
- ANL/NDM-62 Covariance Matrices and Applications to the Field of Nuclear Data by Donald L. Smith, November 1981.
- ANL/NDM-63 On Neutron Inelastic-Scattering Cross Sections of ^{232}Th , ^{233}U , ^{235}U , ^{238}U , ^{239}U , and ^{239}Pu and ^{240}Pu by Alan B. Smith and Peter T. Guenther, January 1982.
- ANL/NDM-64 The Fission-Fragment Angular Distributions and Total Kinetic Energies for $^{235}\text{U}(n,f)$ from 0.18 to 8.83 MeV by James W. Meadows and Carl Budtz-Jørgensen, January 1982.
- ANL/NDM-65 Note on the Elastic Scattering of Several-MeV Neutrons from Elemental Calcium by Alan B. Smith and Peter T. Guenther, March 1982.
- ANL/NDM-66 Fast-neutron Scattering Cross Sections of Elemental Silver by Alan B. Smith and Peter T. Guenther, May 1982.
- ANL/NDM-67 Non-evaluation Applications for Covariance Matrices by Donald L. Smith, July 1982.
- ANL/NDM-68 Fast-neutron Total and Scattering Cross Sections of ^{103}Rh by Alan B. Smith, Peter T. Guenther and James F. Whalen, July 1982.
- ANL/NDM-69 Fast-neutron Scattering Cross Sections of Elemental Zirconium by Alan B. Smith and Peter T. Guenther, December 1982.
- ANL/NDM-70 Fast-neutron Total and Scattering Cross Sections of Niobium by Alan B. Smith, Peter T. Guenther and James F. Whalen, July 1982.
- ANL/NDM-71 Fast-neutron Total and Scattering Cross Sections of Elemental Palladium by Alan B. Smith, Peter T. Guenther and James F. Whalen, June 1982.
- ANL/NDM-72 Fast-neutron Scattering from Elemental Cadmium by Alan B. Smith and Peter T. Guenther, July 1982.
- ANL/NDM-73 Fast-neutron Elastic-Scattering Cross Sections of Elemental Tin by C. Budtz-Jørgensen, Peter T. Guenther and Alan B. Smith, July 1982.
- ANL/NDM-74 Evaluation of the ^{238}U Neutron Total Cross Section by Wolfgang Poenitz, Alan B. Smith and Robert Howerton, December 1982.

- ANL/NDM-75 Neutron Total and Scattering Cross Sections of Elemental Antimony by Alan B. Smith, Peter T. Guenther and James F. Whalen, September 1982.
- ANL/NDM-76 Scattering of Fast-Neutrons from Elemental Molybdenum by Alan B. Smith and Peter T. Guenther, November 1982.
- ANL/NDM-77 A Least-Squares Method for Deriving Reaction Differential Cross Section Information from Measurements Performed in Diverse Neutron Fields by Donald L. Smith, November 1982.
- ANL/NDM-78 Fast-Neutron Total and Elastic-Scattering Cross Sections of Elemental Indium by A. B. Smith, P. T. Guenther, and J. F. Whalen, November 1982.
- ANL/NDM-79 Few-MeV Neutrons Incident on Yttrium by C. Budtz-Jørgensen, P. Guenther, A. Smith and J. Whalen, June 1983.
- ANL/NDM-80 Neutron Total Cross Section Measurements in the Energy Region from 47 keV to 20 MeV by W. P. Poenitz and J. F. Whalen, July 1983.
- ANL/NDM-81 Covariances for Neutron Cross Sections Calculated Using a Regional Model Based on Elemental-Model Fits to Experimental Data by Donald L. Smith and Peter T. Guenther, November 1983.
- ANL/NDM-82 Reaction Differential Cross Sections from the Least-Squares Unfolding of Ratio Data Measured in Diverse Neutron Fields by D. L. Smith, January 1984.
- ANL/NDM-83 The Fission Cross Sections of Some Thorium, Uranium, Neptunium and Plutonium Isotopes Relative to ^{235}U by J. W. Meadows, October 1983.
- ANL/NDM-84 ^{235}U and ^{239}Pu Sample-Mass Determinations and Intercomparisons by W. P. Poenitz and J. W. Meadows, November 1983.
- ANL/NDM-85 Measurement of the $^{51}\text{V}(n,p)^{51}\text{Ti}$ Reaction Cross Section from Threshold to 9.3 MeV by the Activation Method by D. L. Smith, James W. Meadows and Ikuo Kanno, June 1984.

TABLE OF CONTENTS

	<u>Page</u>
ABSTRACT	vi
I. INTRODUCTION	1
II. EXPERIMENTAL PROCEDURES	2
III. DATA ANALYSIS	5
IV. EXPERIMENTAL RESULTS AND DISCUSSION.	7
V. INTEGRAL-DIFFERENTIAL COMPARISONS	9
VI. CONCLUSIONS.	11
ACKNOWLEDGEMENTS.	12
REFERENCES.	13
TABLES	19
FIGURES.	29

ENERGY-DIFFERENTIAL CROSS SECTION MEASUREMENT FOR THE
 $^{51}\text{V}(n,\alpha)^{48}\text{Sc}$ REACTION*

by

Ikuo Kanno**, James W. Meadows and Donald L. Smith

Applied Physics Division
Argonne National Laboratory
9700 South Cass Avenue
Argonne, Illinois 60439
USA

ABSTRACT

The activation method was used to measure cross sections for the $^{51}\text{V}(n,\alpha)^{48}\text{Sc}$ reaction in the threshold region, from 5.515 MeV up to 9.567 MeV. Twenty approximately-monoenergetic cross section values were obtained in this experiment. These data points span the energy region at roughly equal intervals. The experimental resolutions were in the range 0.153 to 0.233 MeV (FWHM). The present differential data cover $\sim 50\%$ of the total integral response of this reaction for the standard ^{235}U thermal-neutron-induced-fission neutron spectrum, and $\sim 44\%$ of the corresponding response for the standard ^{252}Cf spontaneous-fission neutron spectrum. Over the range 7.6 to 9.5 MeV the present experimental cross sections are noticeably larger (e.g., by $\sim 50\%$ at ~ 8.6 MeV) than the corresponding values from the ENDF/B-V evaluation. From ~ 6.7 - 7.5 MeV, the present values are somewhat below those of ENDF/B-V. At still lower energies the agreement is reasonably good considering the uncertainties introduced by energy scale definition very near the effective threshold where the cross section varies rapidly with neutron energy. Calculated integral cross sections based in part on the present work agree reasonably well within errors with reported integral results, provided that the reported data are renormalized to conform with recently-accepted values for appropriate standard reactions.

*This work supported by the U. S. Department of Energy.

**Exchange Associate. Permanent address: Research Reactor Institute, Kyoto University, Kumatori-Cho, Sennan-Gun, Osaka 590-04, Japan.

I. INTRODUCTION

We surveyed CINDA [1] and noted a complete absence of reported differential cross section data for $^{51}\text{V}(n,p)^{51}\text{Ti}$ and $^{51}\text{V}(n,\alpha)^{48}\text{Sc}$ below ~ 10 MeV. Since ^{51}V is the dominant isotope (99.750% abundance) of elemental vanadium [2], the absence of such data has serious implications for the development of reliable evaluated neutron cross section files for vanadium. Two major evaluations (ENDF/B-V, U.S.A. [3] and JENDL-2, Japan [4]) were recently generated for vanadium (n,p) and (n, α) without experimental guidance in the threshold regions. These cross section evaluations employed model calculations which extrapolated to threshold from the available higher-energy experimental results. It is well known that such extrapolations produce results of dubious reliability, owing to uncertainties stemming from imperfect understanding of the reaction mechanisms, model limitations, and the rudimentary status of knowledge of important model parameters such as level densities [5]. The (n,p) and (n, α) reactions for vanadium are of importance for nuclear-energy applications, so there are several requests for measurements (e.g., Refs. 6 and 7). The primary concern involves material damage occurring in vanadium-bearing structures of reactors when they experience high fluences of fast neutrons. Neutron-radiation-induced hydrogen and helium production has been related to phenomena such as embrittlement and swelling of the afflicted structures (e.g., Ref. 8). While it is unrealistic to anticipate that (n,p) and (n, α) cross sections will be comprehensively measured for all the elements, over wide energy ranges, in the foreseeable future, there is clearly a need to establish a larger and more reliable data base than now exists, especially for materials of particular applied importance and for the refinement of nuclear modeling techniques.

Because of the applied needs, it was decided to measure the $^{51}\text{V}(n,p)^{51}\text{Ti}$ and $^{51}\text{V}(n,\alpha)^{48}\text{Sc}$ reaction energy-differential cross sections. The activation method was selected since it was expected to be reliable in these instances owing to the favorable and well-known decay characteristics of ^{51}Ti and ^{48}Sc . Our results for the (n,p) reaction were recently reported [9]. This work confirmed our previously-held suspicions concerning poor reliability to be expected when model calculations are used for producing evaluated cross sections of this nature. In fact, large differences were discovered between the measured $^{51}\text{V}(n,p)^{51}\text{Ti}$ cross sections and those predicted by both ENDF/B-V [3] and JENDL-2 [4]. The present report presents the results of our corresponding experimental investigation of the (n, α) reaction. The goal of the present experiment was to measure the $^{51}\text{V}(n,\alpha)^{48}\text{Sc}$ reaction cross section over a reasonably-wide energy range. Section II describes the experimental method used. Section III deals with details of the data analysis, including a comprehensive treatment of experimental errors. The results are reported in Section IV, where comparison is also made with other monoenergetic experimental data (all above 10 MeV) and with two existing evaluations for the vanadium (n, α) reaction. Section V discusses a comparison we have made between available differential and integral results for

two widely-encountered fission-neutron spectra. Finally, our conclusions appear in Section VI.

II. EXPERIMENTAL PROCEDURES

The $^{51}\text{V}(n,\alpha)^{48}\text{Sc}$ reaction is amenable to measurement via the activation method. The isotopic abundance of ^{51}V in elemental vanadium is 99.750%, with ^{50}V as the small remaining isotopic constituent [2]. The reaction Q-value is -2.055 MeV [2]. The decay half life of ^{48}Sc is 43.67 ± 0.09 h [2], a very convenient value for routine activation studies. ^{48}Sc decays via β^- emission to excited levels in ^{48}Ti , and they subsequently decay to the ground state by gamma-ray emission with the following dominant transitions: 0.984 MeV ($100.0 \pm 0.3\%$), 1.037 MeV ($97.5 \pm 0.3\%$), and 1.312 MeV ($100.0 \pm 0.3\%$) [2]. The indicated branching factors represent the percentages of ^{48}Sc decays where each specific gamma ray is observed. These gamma rays have convenient energies for detection with a Ge(Li) spectrometer. The only complication encountered in analysis of the decay of ^{48}Sc corresponds to sum-coincidence losses. More will be said about how this was handled later in this section.

The samples were metallic vanadium disks averaging 0.330 cm in thickness and 2.557 cm in diameter. The vanadium content was $99.8 \pm 0.2\%$ by weight. The dominant impurities were Al, Si, Cr and Fe, but none of these gave problems insofar as the present experiment was concerned. The sample density was measured as 5.92 ± 0.04 g/cm³.

Nearly monoenergetic neutrons for the irradiations were produced by bombarding thin targets with monoenergetic charged-particle beams from the Argonne National Laboratory Fast-Neutron Generator (FNG) Facility [10,11]. All measurements were performed with the $^2\text{H}(d,n)^3\text{He}$ reaction, using a gas target as described in Refs. 12 and 13. The target assembly is also pictured schematically in Fig. 1 of Ref. 9. This target was required to dissipate up to 100 watts of beam power during operation. The target assembly itself was water cooled, and an air jet directed at the gas cell was used as well. The neutron energy was controlled by selecting the appropriate incident deuteron energy since the source reaction is a two-body interaction with a well-defined Q-value. This source reaction suffers interference from the $^2\text{H}(d,np)^2\text{H}$ reaction at higher energies, and thus ceases to be truly monoenergetic [12]. Methods for coping with this problem have been described previously [12,14,15]. The deuteron beam from the FNG accelerator was magnetically analyzed, and the energy-scale calibration was based upon observation of the well-known $^7\text{Li}(p,n)^7\text{Be}$, $^{11}\text{B}(p,n)^{11}\text{C}$ and $^{27}\text{Al}(p,n)^{27}\text{Si}$ reaction thresholds [16,17]. These calibration measurements were performed in a separate experiment involving proton beams. Although the incident deuteron energies are believed to be known to within better than ± 5 keV over the entire energy range of this experiment, the average neutron energies are less well known, primarily due to uncertainties in calculating target energy losses for deuterons in the

gas target. Thus, the average neutron energies reported in this work are conservatively estimated to be uncertain by about 20% of the full-width-half-maximum (FWHM) resolutions for the incident-neutron-energy distributions, i.e., by ~ 31 - 47 keV.

The vanadium sample disks were placed perpendicular to the incident deuteron beam (at zero degrees) at a distance of 3.47 cm from the target for all the irradiations. The samples were attached to a low-mass fission detector monitor as shown in Fig. 1 of Ref. 9. This detector is a parallel-plate ionization chamber used to detect fission fragments emitted from a thin deposit of uranium. The chamber has 0.025 -cm-thick steel walls, and the chamber electrode and uranium deposit backing are 0.025 -cm-thick steel disks. Methane (CH_4) at atmospheric pressure is the filler gas. The uranium deposit is a thin, uniform film of depleted uranium (effectively 100% ^{238}U) 2.54 -cm in diameter, amounting to $5.012 \times 10^{18} (\pm 2\%)$ atoms. Procedures for making and calibrating this deposit have been previously described [18-20].

Activity measurements for ^{48}Sc were achieved by counting the emitted 0.984 -, 1.037 - and 1.312 -MeV gamma rays with a Ge(Li) detector having an active volume of ~ 100 cm³. Counting deadtime corrections were small, and they were deduced for each sample count using information recorded during these runs. Each sample was counted in a well-defined position close to this detector. Determination of an appropriate counting efficiency for this configuration was an essential part of the experiment. Three independent methods were used, and they all produced results in good agreement with each other. The final efficiency used in the cross section calculations was based on one method alone, and this is described below in some detail. The two other methods served to confirm the first result, and they are discussed rather briefly below as well.

The primary calibration method used is similar to the approach we used earlier for the $^{51}\text{V}(n,p)^{51}\text{Ti}$ experiment [9]. First, a second reproducible counting position was established ~ 20 cm from the detector (on the detector axis). One vanadium sample was irradiated for a sufficiently long time at a high neutron energy to produce adequate ^{48}Sc activity for counting in both of the positions mentioned above. All the other samples irradiated in this experiment were oriented in the same fashion as this calibration sample so that activity nonuniformity effects would cancel to first order. These effects were small anyway. Measurements of full-energy peak count rates for the calibration sample yielded a ratio of the counting efficiencies at the two positions to $\sim 0.6\%$ accuracy. Further calibration effort was then directed toward the distant position. Standard sources [21-23] were used to establish the bare-point-source gamma-ray efficiency curve for full-energy peaks versus gamma-ray energy at this distant position. Calculations were then performed to modify this efficiency curve to an equivalent curve representing the same activity distributed in an extended absorbing medium of vanadium representing a typical sample. Thus, the counting efficiencies

for each γ -ray peak (0.984-, 1.037- and 1.312 MeV) from ^{48}Sc were deduced indirectly for the close-in counting position actually used in the experiment. This method avoids the problem of sum-coincidences. Since they are negligible for the distant calibration position, the close-in sum coincidence corrections are automatically included in the explicit near-to-far position efficiency ratios for each gamma ray from ^{48}Sc , measured as described above. In order to improve the statistics for routine sample counts, the yields of the three dominant peaks indicated above were actually summed. Based on the analysis described above, our effective detection efficiency (inclusive of the gamma-ray branching factor), which corresponded to the yield of the three summed transitions in the routine close-in counting position, was 0.0408 ($\pm 1\%$).

Our second calibration method actually exploited the fact that sum-coincidence peaks were present in the spectra for the close-in counting position. A single-detector sum-peak coincidence method was used to establish the efficiencies for each of the three dominant gamma-ray lines [24]. The average ratio of the efficiencies derived by this method to the corresponding single-transition efficiencies derived by the method described in the preceding paragraph was 1.02 ± 0.01 , which indicates consistency for the two methods within the errors. To provide an additional check on the efficiency, two samples which had been irradiated in our laboratory were counted several times here and were then sent to be counted at Physikalisch-Technische Bundesanstalt (PTB), Federal Republic of Germany [25]. Each laboratory then derived the effective disintegration rates for these samples, time corrected to a selected zero time, based on independent calibrations at the respective laboratories. For one sample our calibration yielded a disintegration rate 0.4% larger than found by PTB, while for the second sample, our result was 1.1% smaller. This comparison relates to our primary calibration method, and the excellent agreement exceeds expectations based on our estimated error of $\sim 1.2\%$ and an equivalent error for the PTB measurement. Thus, the assumed 1% error in the gamma-ray detector efficiency we quote appears to be reasonable. We also measured sample count rates versus orientation of the sample and found that the difference between the two possible orientations in the normal close-in position was $(0.6 \pm 0.4\%)$. Since the sample counting and detector calibration were conducted with a consistent sample-orientation convention, as indicated above, no correction is needed for this small effect. Any activity nonuniformity observed in the counting would be due primarily to geometric effects resulting from the sample being placed quite close to the extended-line neutron source during the irradiations.

The sample irradiation times all exceeded one hour and some runs were as long as 13 hours. The neutron output rates during these measurements were monitored and found to be essentially constant. Long counters and a beam current integrator served as auxiliary monitors during all these irradiations. Background measurements were made at each energy to provide information on the effect of neutrons produced from deuteron bombardment of the target-cell structure. Corrections to the fission-monitor data were obtained for each such energy. However, it was established that the pro-

duction of ^{48}Sc in the sample was significant only at the higher deuteron energies, so no background sample irradiations were performed at lower energies. Previous experience has indicated that most of the background neutrons come from (d,n) reactions with the 3.2-mg/cm^2 nickel-foil cell entrance window or with impurities which tend to build up on the target [11]. The background is known to vary with time. Therefore, for the longer runs two background measurements were made, one before and one after the main run, and the results were averaged. This investigation of background effects indicated that the background fissions varied between 2-26% while the background ^{48}Sc production was $< 2\%$ at all energies.

For some of the measurements, the ^{48}Sc decay gamma-ray peaks were not particularly prominent relative to the overall detector background. Therefore, this background was carefully measured and no gamma-ray lines were found which might interfere with the ^{48}Sc counting. To be certain that all the yield in the 0.984-, 1.037- and 1.312-MeV lines came from ^{48}Sc , a careful measurement of the decay half life of the summed yield for these lines was performed. The result of this analysis was a measured half life of 43.79 ± 0.22 h which agrees very well with the value 43.67 ± 0.09 h from the literature [2].

III. DATA ANALYSIS

The experimental data were analyzed using the same general methods described in Refs. 12 and 26. The first step was a determination of the 0.984-, 1.037- and 1.312-MeV gamma-ray peak yields. The individual peak yields were then summed and errors for these sums were evaluated. Utilizing parameters of the individual irradiation histories, corrections for ^{48}Sc activity decay were applied. These results, when combined with the measured Ge(Li) detector efficiency, yielded values for the total number of ^{48}Sc atoms produced in each irradiated sample. These data were also corrected for the effect of background neutrons from the empty target cell.

Next, we examined the fission-monitor data. An extrapolation correction was applied to account for fission events of low-energy which were masked by the alpha-particle and noise pulses. For the present experiment this correction was independently derived for each data point. The magnitudes of these corrections were typically $\sim 3\%$. Fission fragments emitted near 90° in the uranium deposit cannot escape and are thus not recorded. This effect is somewhat energy-dependent and it also depends upon the fragment angular distributions. The most significant dependence is upon the deposit thickness. Using fragment angular distribution data from Ref. 27, we found that corrections of $\sim 3\text{-}4\%$ were required. As indicated in Section II, corrections for fissions produced by background neutrons were applied. These corrections were also measured for each data point.

Neutron-multiple-scattering corrections for this experiment could not be measured and thus had to be calculated. The basic concept is described

in Ref. 26, but the calculational procedure has since been improved and is further described in Ref. 28. The scattering corrections are sufficiently small, in experiments such as the present one, so that the correction procedure need only consider additional events produced by once-scattered neutrons. However, both elastic and inelastic scattering contributions are included. The scattering-correction parameters were calculated at several neutron energies using ENDF/B total, scattering and reaction cross sections [3]. The results appear in Table 1. Required values for intermediate energies were derived from this table by interpolation. Lower-energy values were estimated by extrapolating the 6.268-MeV correction values. There is some cancellation in the effects of these scattering parameters since this is basically a ratio experiment. The net correction, however, remains in the range 5.5-7% over the energy range of this experiment.

The corrected fission and activity data, and calculated scattering corrections, were used to compute $^{51}\text{V}(n,\alpha)^{48}\text{Sc}$ cross sections. The calculations were performed with a computer code which determined a number of additional corrections involving geometry factors, neutron source properties, neutron absorption, etc. Again, the procedure is basically the one described in Refs. 12 and 26; however, it has been refined to incorporate concepts described in Ref. 14. These newer features deal primarily with the way the average neutron energy and neutron-energy resolution are calculated. As for the earlier $^{51}\text{V}(n,p)^{51}\text{Ti}$ work [9], this is an important consideration since the (n,α) cross section is strongly energy dependent near threshold.

Corrections for secondary-neutron groups from the source reaction are a matter of concern. The $^2\text{H}(d,np)^2\text{H}$ reaction produces a continuous breakup-neutron spectrum [11,12]. Neglect of this breakup-group correction would lead to an error of as much as 10.5% at the highest energy of the experiment. However, the breakup correction was calculated and applied to our data so the residual uncertainty is estimated to be $< 2\%$. When the gas target heats up, the density of the gas in the cell decreases [13]. This feature alters the effective energy resolution and leads to slightly higher average neutron energies. We took this effect into consideration in analyzing the data from the present experiment. In the worst case, a shift of < 15 keV toward higher average neutron energy resulted.

We have estimated the principal error sources for this experiment, including correlations, using methods described in Refs. 29 and 30. The objective of this effort is provision of sufficient uncertainty information so that a complete data covariance matrix can be generated for evaluation applications (e.g., see Ref. 29).

Seven sources of random error and twelve sources of systematic error were considered. These are identified briefly in Table 2, and the ranges of values we estimate appear there as well. Errors and correlations for the $^{238}\text{U}(n,f)$ standard cross section have to be considered separately, not as

part of the present analysis. Twenty distinct cross section ratios were obtained in the present work. Each of these values is identified by a data point number. Table 3 provides explicit estimated magnitudes for the variable error components identified in Table 2. Table 4 indicates the correlations we believe exist between systematic errors in the same category for the various data points. No cross-category correlations are expected for these data. Some additional comments are in order regarding certain of these error components. Random component R_4 for the extrapolation correction is based on the assumption that the magnitude of the error is $\sim 25\%$ of the correction; this appears to be consistent with the observed scatter in the individually-determined corrections. The same can be said for systematic error component S_4 which deals with the uranium-deposit-thickness correction. The systematic error component S_{10} is derived by assuming that each of the calculated scattering correction parameters α, β, γ and ρ (see Ref. 26) has an uncertainty of $\sim 20\%$. The uncertainty in the net correction η (see Table 1) is calculated by standard error propagation techniques (see Ref. 29), assuming the partial correction factor errors to be uncorrelated. Typically, the uncertainty in the net scattering correction η then amounts to $\sim 30\%$ of the correction. The neutron-energy-difference dependence of the correlations for systematic error components S_8 and S_{10} , expressed in Table 4, is simply a plausible assumption, reflecting the fact that the corrections for data points nearby in energy are believed to be more strongly correlated than those widely separated in energy. Systematic error component S_{12} can be estimated only when knowledge of the cross section excitation function shape and of the energy scale uncertainty is available. Energy scale uncertainty, as indicated previously, is assumed to be $\sim 20\%$ of the FWHM resolution. Shape sensitivity parameters ($\partial\sigma/\partial E$) were deduced mainly from an eyeguide to our experimental results. Further discussion on this eyeguide appears in Section V.

IV. EXPERIMENTAL RESULTS AND DISCUSSION

The isotopic, energy-dependent $^{51}\text{V}(n,\alpha)^{48}\text{Sc}$ cross section values from this experiment are presented in Table 5. We emphasize the experimental ratios and corresponding errors since these are obtained directly from the measurements. However, (n,α) cross sections were derived readily from these ratios by using ENDF/B-V [3] evaluated cross sections for the standard ^{238}U fast-neutron-fission reaction. The overall uncertainty in the derived (n,α) cross section is obtained by combining the ratio and standard errors in quadrature. A ratio-data covariance matrix can be calculated from information given in Tables 2-5, using methods described in Ref. 29. We have performed this analysis and provide our results in the form of a dimensionless correlation matrix in Table 6. In order to obtain an (n,α) cross section covariance matrix, the ratio covariance matrix would have to be combined with the ^{238}U -fission-cross-section covariance matrix, deduced from the appropriate ENDF/B-V File 33 entry [3], using the method described in Ref. 29.

Comparisons are made between the present experimental results and experimental and evaluated values from the literature in Figs. 1-3. The present data cover a range of more than three orders of magnitude in cross section and provide detailed definition of the threshold region for this reaction (see Figs. 1-3). These results, however, are not directly comparable with experimental values we obtained from the literature [1,31-53] since all of our values are below 10 MeV while the available reported differential data are at energies above 10 MeV. Owing to the large number of data points in the literature, and the compressed scales used in preparing Figs. 1 and 3, it is difficult to distinguish individual data points on these figures. Therefore, we also plotted the data above 10 MeV using a scale which exhibits the results in greater detail (see Fig. 4). We have chosen to compare the available data, including the present values, with two recent evaluations, namely ENDF/B-V [3] and JENDL-2[4], in Figs. 1-4. The evaluated cross sections are for elemental vanadium, but the 0.25% difference between the elemental-vanadium and ^{51}V -isotopic values is probably negligible at most energies. A possible exception could be in the extreme threshold region. Here, the effect of the $^{50}\text{V}(n,\alpha)^{47}\text{Sc}$ reaction may be noticeable since it has a Q value of + 0.757 MeV, and thus a considerably-lower probable effective threshold than the corresponding ^{51}V reaction. Of special interest to us is the comparison of our experimental results with ENDF/B-V [3] since this evaluation is important for the U.S. nuclear-energy-technology programs. The agreement of ENDF/B-V with the present experimental results is quite good below ~ 7.5 MeV. However, in the energy range from $\sim 8-9$ MeV, our values differ considerably from ENDF/B-V. Fig. 2 illustrates this point graphically. We will see in Section V that this difference is significant for fission reactor applications since the integral response curves for $^{51}\text{V}(n,\alpha)^{48}\text{Sc}$ in typical fission-neutron spectra peak in this energy region. The present measured differential cross sections are $\sim 50\%$ larger than ENDF/B-V around 8.5 MeV. A similar situation occurs for the (n,p) cross sections (see Ref. 9). Our experimental data appear to be lower from 7-9 MeV and higher above 9 MeV than the JENDL-2 evaluation [4]. Although the situation above 10 MeV is only indirectly relevant to the present investigation, the JENDL-2 evaluation [4] appears to represent most of the higher-energy experimental cross section data far better than ENDF/B-V [3]. This fact is of interest for our integral/differential data comparison which is discussed in Section V.

Over much of the energy range of this experiment, the errors in the measured ratios are $\sim 6-9\%$ while the derived cross section errors are $\sim 7-10\%$. At the lower energy range, the statistical errors in the measured ^{48}Sc activity and the systematic errors attributed to neutron-energy uncertainty are dominant. It is evident from Table 5 and Fig. 1 that the outcome of tests to determine the reproducibility of several measured values was satisfactory.

V. INTEGRAL-DIFFERENTIAL COMPARISONS

While no experimental monoenergetic data have been reported for $^{51}\text{V}(n,\alpha)^{48}\text{Sc}$ in the energy region addressed by the present experiment, some integral results have been measured and they can be used indirectly to test our results. Two standard neutron spectra commonly used to test differential data are the ^{235}U thermal-neutron-induced-fission neutron spectrum and the ^{252}Cf spontaneous-fission neutron spectrum [54]. ^{252}Cf sources can be made to be very compact with only small perturbations by the encapsulation material. Consequently, the spectra from such sources can be very well characterized in principle, and considerable recent effort has been devoted to the task of standardizing this neutron field (e.g., see Refs. 55-59). It is far more difficult to produce and characterize the standard ^{235}U thermal-neutron-induced-fission neutron spectrum [60]. In the present analysis we rely on the ENDF/B-V [3] representation. In actual fact, integral measurements are rarely performed in pure uranium-fission neutron spectra; instead results are reported for a variety of fission-reactor spectra. While the detailed spectrum shape has an important influence on the absolute fission-spectrum-average cross section, it has been observed that the shapes of the high-energy tails of fission-reactor spectra are quite similar to that of a pure ^{235}U -fission spectrum. Thus, the integral cross section ratio for two reactions with reasonably similar thresholds tends to be relatively insensitive to the particular type of fission reactor. Thus by considering only measured reactor-spectrum reaction-rate ratios of unknown reactions to standard reactions it is possible to compare seemingly rather diverse experimental results. This concept is discussed in some detail by Winkler et al. [61].

It was necessary to pursue this approach here since an examination of the available fission-spectrum integral data (e.g., see CINDA [1]) indicated diverse origins for the potentially-comparable $^{51}\text{V}(n,\alpha)^{48}\text{Sc}$ results. Only one ^{252}Cf -spectrum-average result has been reported [62]. Several reactor-fission-spectrum results are presently available [63-67]. We have listed these experimental values in Table 7, as quoted in the literature. Furthermore, we have identified in each case a suitable standard reaction which was also investigated by the original authors in their work. Whenever possible we referred to reported values from these experiments for $^{27}\text{Al}(n,\alpha)^{24}\text{Na}$, which is one of the best-known standard reactions from the ENDF/B-V Dosimetry File [3]. It has a threshold in the several-MeV range, thereby minimizing sensitivity to differences in the reactor spectrum shapes. We used values for this standard integral cross section which are consistent with ENDF/B-V [3,68,69], and then renormalized the $^{51}\text{V}(n,\alpha)^{48}\text{Sc}$ integral cross sections quoted in the original literature sources according to the method described by Winkler et al. [61]. An exception was our choice of the value from Winkler et al. [61] for $^{63}\text{Cu}(n,\alpha)^{60}\text{Co}$. It served as the standard for renormalizing the data of Dudgey and Heinrich [64] since Winkler et al. have shown that ENDF/B-V is not a particularly good representation for

$^{63}\text{Cu}(n,\alpha)^{60}\text{Co}$. In all of these renormalizations it was assumed that differences attributable to decay constants and other experimental details could be ignored. The results of this analysis also appear in Table 7. We take the original errors given by the authors, and then simply convert these to proper renormalized values. No estimates of uncertainties due to the renormalization process, or due to the standard cross sections, were considered. Thus, the errors in the renormalized values can be considered as minimum uncertainties.

In order to provide a comparison of measured and calculated fission-spectrum average results, it was necessary to generate a differential curve which represented our best current knowledge of the (n,α) cross section for ^{51}V , based on available differential information including the present results. We did not perform a rigorous evaluation. The curve we generated is based upon: i) the ENDF/B-V evaluation [3] for neutron energies below 5.8 MeV, ii) an eyeguide to the present experimental results in the range 5.8 - 9.6 MeV, iii) the ENDF/B-V evaluation from 9.6 - 11 MeV, and the JENDL-2 evaluation [4] for energies from 11-20 MeV. Table 8 contains the numerical values for this hybrid curve, $\sigma(E)$. This curve is compared with all available experimental data in Fig. 5. In the present analysis, we rely on the standard ENDF/B-V [3] representation of the ^{235}U thermal-neutron-induced-fission neutron spectrum. For the ^{252}Cf spontaneous-fission neutron spectrum, we employed a representation based on Refs. 55 and 56. The relationship between the integral cross sections $\langle\sigma\rangle$, the differential cross section $\sigma(E)$ and the spectrum $\phi(E)$ is expressed by the equation

$$\langle\sigma\rangle = \frac{\int_0^{20 \text{ MeV}} \sigma(E)\phi(E)dE}{\int_0^{20 \text{ MeV}} \phi(E)dE} \quad (1)$$

Owing to the nature of $\phi(E)$ and $\sigma(E)$, the response range is limited essentially to neutron energies between ~ 6 -18 MeV for $^{51}\text{V}(n,\alpha)^{48}\text{Sc}$. The method of analysis is described in Ref. 70. Our investigation was limited to the ^{235}U and ^{252}Cf standard fission spectra, for $\phi(E)$, and to ENDF/B-V [3], JENDL-2 [4] and the hybrid curve defined in Table 8, for $\sigma(E)$. The calculated spectrum-average cross sections for $^{51}\text{V}(n,\alpha)^{48}\text{Sc}$ appear in Table 9. Following the approach from Ref. 70, the graphical material from our spectral-response analyses for $\sigma(E)$ from Table 8 appears in Figs. 6 and 7, for ^{235}U and ^{252}Cf respectively. The principal results from Tables 7 and 9 are summarized in Figs. 8 and 9 for the ^{235}U and ^{252}Cf fission-neutron spectra, respectively. Here, measured and calculated $\langle\sigma\rangle$ are compared. Our calculated $\langle\sigma\rangle$, using Table 8 values for $\sigma(E)$, are represented in each figure by the solid vertical line. The dashed lines represent $\pm 7\%$ uncertainty in these values, corresponding to the estimated minimum uncertainties. It is seen that the agreement between differential and integral results is reasonably good. Since our data span only $\sim 50\%$ of the response range, the higher-energy results are of equal consequence in this context. Although ENDF/B-V [3] apparently underestimates $\sigma(E)$ in the important response range from 7.5-9.5 MeV, it also overpredicts

the cross sections from ~ 13 -20 MeV. Thus $\langle\sigma\rangle$ for ENDF/B-V does not differ greatly from the result based on Table 8. The main problem with JENDL-2 [4] appears to be < 9 MeV. In fact, uncertainty about how exactly to represent $\sigma(E)$ near threshold for the JENDL-2 evaluation [4] led to difficulties in calculating $\langle\sigma\rangle$ values. It was noticed that the numerical values in the JENDL-2 file indicate considerably larger cross sections between ~ 2.1 and 9.0 MeV than are shown in a corresponding figure from Ref. 4. Since the latter appears more realistic, we chose to use values read from that figure for the present analysis. Therefore, the values corresponding to JENDL-2 in Table 9 and Figs. 8 and 9 may be in error if we have misrepresented this evaluation.

The importance of having detailed knowledge of $\sigma(E)$ is illustrated by the situation for ENDF/B-V. Here, a curve for $\sigma(E)$ which clearly misrepresents the differential data rather badly in two energy ranges leads to calculated $\langle\sigma\rangle$ which are in reasonable agreement with integral data, fortuitously.

VI. CONCLUSIONS

The present measurements provide unique differential cross section data in the important threshold region for the $^{51}\text{V}(n,\alpha)^{48}\text{Sc}$ reaction. The results are relevant to the needs of applied nuclear-energy programs, especially for fusion where vanadium is considered to be an important structural material. The present data cover $\sim 50\%$ of the integral response range, and a differential/integral comparison based on our data and a reasonable representation for the higher-energy cross section led to quite-acceptable agreement considering the uncertainties involved.

This work re-emphasizes the general conclusion discussed in our earlier investigation of the $^{51}\text{V}(n,p)^{51}\text{Ti}$ reaction [9], namely that the state of the art in nuclear-model calculations is such that, in general, one cannot expect to calculate (n,X) reaction cross sections (even the shapes) with much quantitative certainty. Typically, discrepancies between model calculations and data (provided that the calculations are not adjusted to explicitly fit the data) of the order of 20-50% are typical. This certainly seems to be the case for $^{51}\text{V}(n,p)^{51}\text{Ti}$ [9] and $^{51}\text{Ti}(n,\alpha)^{48}\text{Sc}$ (present work). The origins of this uncertainty cannot be identified, in general, as originating predominantly from parameter uncertainties or from basic model flaws. Clearly, more work is needed to improve the reliability of model predictions since not all reaction cross sections can be as conveniently measured as $^{51}\text{V}(n,p)^{51}\text{Ti}$ and $^{51}\text{V}(n,\alpha)^{48}\text{Sc}$. A solid base of reliable experimental (n,X) reaction cross section data is clearly needed to provide "benchmarks" for testing nuclear-model calculational techniques. Our investigations of $^{51}\text{V}(n,p)^{51}\text{Ti}$ [9] and $^{51}\text{V}(n,\alpha)^{48}\text{Sc}$ (present work) contribute toward this objective.

ACKNOWLEDGEMENTS

This work was supported by the U.S. Department of Energy. One of the authors (I.K.) gratefully acknowledges support provided by the American Nuclear Society International Student Exchange Program. The cooperation of W. Mannhart from Physikalisch-Technische Bundesanstalt (PTB), Federal Republic of Germany, in intercomparing gamma-ray detector calibrations for this experiment, is greatly appreciated by the authors. The authors are also indebted to K. Kobayashi for his helpful suggestions and for assistance in certain aspects of this work.

REFERENCES

1. CINDA-A (1935-1976) Vol. I- June 1979; CINDA-83 (1977-1983) - May 1983; CINDA-83 Supplement-October 1983: An Index to the Literature on Microscopic Neutron Data," International Atomic Energy Agency, Vienna, Austria.
2. Table of the Isotopes, 7th Edition, C. Michael Lederer and Virginia S. Shirley, Eds., John Wiley and Sons, Inc., New York (1978).
3. "Evaluated Neutron Data File, ENDF/B", National Nuclear Data Center, Brookhaven National Laboratory, Upton, New York 11973, USA. Reference is made in the present work to both the ENDF/B-IV and -V versions of this file.
4. Shigeya Tanaka, "Evaluation of Neutron Cross Sections for Vanadium," JAERI-M-82-151, Japan Atomic Energy Research Institute, Tokai-mura, Naka-gun, Ibaraki-ken 319-11, Japan.
5. Robert C. Haight, "Applied Uses of Nuclear Level Densities," in "Proceedings of an Advisory Group Meeting on Basic and Applied Problems of Nuclear Level Densities," Brookhaven National Laboratory, April 11-15, 1983. Ed. M. Bhat, BNL-NCS-51094, National Nuclear Data Center, Brookhaven National Laboratory, Upton, New York 11973 (1983).
6. E. T. Cheng, D. R. Mathews and K. R. Schultz, "Magnetic Fusion Energy Program Nuclear Data Needs," GA-A16886, General Atomic Company, P. O. Box 81608, San Diego, California 92138 (1982).
7. "Compilation of Requests for Nuclear Data," compiled and edited by the National Nuclear Data Center for the DOE Nuclear Data Committee, BNL-NCS-51572, Brookhaven National Laboratory, Upton, New York 11973 (1983).
8. Donald L. Smith, "Neutron Dosimetry for Radiation Damage in Fission and Fusion Reactors," in "Proceedings of an International Conference for Nuclear Cross Sections for Technology," University of Tennessee, Knoxville, Tennessee, October 22-26, 1979, Eds. J. L. Fowler, C. H. Johnson and C. D. Bowman, NBS Special Publication 594, National Bureau of Standards, U. S. Department of Commerce, Washington, D.C., p. 285 (1980).
9. Donald L. Smith, James W. Meadows and Ikuo Kanno, "Measurement of the $^{51}\text{V}(n,p)^{51}\text{Ti}$ Reaction Cross Section from Threshold to 9.3 MeV by the Activation Method," ANL/NDM-85, Argonne National Laboratory, Argonne, Illinois 60439, USA (1984).

10. S. A. Cox and P. R. Hanley, IEEE Trans. Nucl. Sci. 18, 108 (1971).
11. James W. Meadows and Donald L. Smith, "Neutron Source Investigations in Support of the Cross Section Program at the Argonne Fast-Neutron Generator," ANL/NDM-53, Argonne National Laboratory, Argonne, Illinois 60439 (1980).
12. D. L. Smith and J. W. Meadows, "Method of Neutron Activation Cross Section Measurement for $E_n = 5.5-10$ MeV Using the $D(d,n)^3\text{He}$ Reaction as a Neutron Source," ANL/NDM-9, Argonne National Laboratory, Argonne, Illinois 60439 (1974).
13. James W. Meadows, Donald L. Smith and Gerhard Winkler, Nucl. Instr. and Meth. 176, 439 (1980).
14. Donald L. Smith, "Some Comments on Resolution and the Analysis and Interpretation of Experimental Results from Differential Neutron Measurements," ANL/NDM-49, Argonne National Laboratory, Argonne, Illinois 60439 (1979).
15. Donald L. Smith, "A Least-Squares Method for Deriving Reaction Differential Cross Section Information from Measurements Performed in Diverse Neutron Fields," ANL/NDM-77, Argonne National Laboratory, Argonne, Illinois 60439 (1982).
16. E. H. Beckner, R. L. Bramblett, G. C. Phillips and T. A. Eastwood, Phys. Rev. 123, 2100 (1961).
17. J. B. Marion, Rev. Mod. Phys. 38, 660 (1966).
18. J. W. Meadows, Nucl. Sci. Eng. 49, 310 (1972).
19. Donald L. Smith and James W. Meadows, "Response of Several Threshold Reactions in Reference Fission Neutron Fields," ANL/NDM-13, Argonne National Laboratory, Argonne, Illinois 60439 (1975).
20. W. P. Poenitz, J. W. Meadows and R. J. Armani, " ^{235}U Fission Mass and Counting Comparison and Standardization," ANL/NDM-48, Argonne National Laboratory, Argonne, Illinois 60439 (1979).
21. Standard ^{152}Eu Gamma Calibration Source, Type EGMA 3, No. 5243, Laboratoire de Metrologie des Rayonnements Ionisants, Commissariat a l'Energie Atomique, Saclay, BP No. 2, 91190 Gif sur Yvette, France.
22. Mixed-Radionuclide Point-Source Standard, No. SRM 4275-140, National Bureau of Standards, Washington, D.C. 20234, U.S.A.
23. ^{60}Co Point-Source Standard, No. SRM 4210-3, National Bureau of Standards, Washington, D.C. 20234, U.S.A.

24. James W. Meadows and Donald L. Smith, "Gamma-Ray Detector Calibration Methods Utilized in the Argonne FNG Group Activation Cross Section Measurement Program," ANL/NDM-60, Argonne National Laboratory, Argonne, Illinois 60439, U.S.A. (1984).
25. W. Mannhart, Physikalisch-Technische Bundesanstalt, Postfach 3345, 3300 Braunschweig, Federal Republic of Germany, private communication (1983).
26. Donald L. Smith and James W. Meadows, "Measurement of $^{58}\text{Ni}(n,p)^{58}\text{Co}$ Reaction Cross Sections for $E_n=0.44-5.87$ MeV Using Activation Methods," ANL-7989, Argonne National Laboratory, Argonne, Illinois 60439 (1973).
27. J. E. Simons and R. L. Henkel, Phys. Rev. 120, 198 (1960).
28. D. L. Smith and J. W. Meadows, "Neutron Inelastic Scattering Studies for Lead-204," ANL/NDM-37, Argonne National Laboratory, Argonne, Illinois 60439 (1977).
29. Donald L. Smith, "Covariance Matrices and Applications to the Field of Nuclear Data," ANL/NDM-62, Argonne National Laboratory, Argonne, Illinois 60439 (1981).
30. Donald L. Smith, "Non-Evaluation Applications for Covariance Matrices," ANL/NDM-67, Argonne National Laboratory, Argonne, Illinois 60439 (1982).
31. D. Crumpton, J. Inorg. Nucl. Chem 31, 3727 (1969).
32. A. Paulsen, R. Widera and H. Liskien, Atomkernenergie 22, 291 (1974).
33. W. H. Warren and W. L. Alford, Ann. Nucl. Energy 9, 369 (1982).
34. J. C. Robertson, B. Audric and P. Kolkowski, Journal of Nuclear Energy 27, 531 (1973).
35. E. T. Bramlitt and R. W. Fink, Phys. Rev. 131, 2649 (1963).
36. S. Qaim, "Proc. of a Specialist's Meeting on Neutron Data of Structural Materials for Fast Reactors," CBNM, Geel, Belgium, 5-8 December 1977.
37. V. O. Schwerer et al., Oesterr. Akad. Wiss., Math. + Naturw. Anzeiger 113, No. 9, 153 (1976). Data obtained from Computer Files on Microscopic Neutron Data, EXFOR 20811.004, International Atomic Energy Agency, Vienna, Austria.
38. M. Borman, S. Cierjacks, R. Langkau, H. Neuert and H. Pollehn, Le Journal de Physique et le Radium 22, 602 (1961).

39. M. Hillman, Nucl. Phys. 37, 78 (1962).
40. H. Vonach, Oesterr. Akad. Wiss., Math. + Naturw. Anzeiger 95, 199 (1958).
41. W. Mannhart and H. Vonach, Zeitschrift fuer Physik A272, 279 (1975).
42. H. K. Vonach, W. G. Vonach, H. Muenzer and P. Schramel, "Proc. Conf. on Neutron Cross Sections and Technology," Washington, D.C., p. 886 (1968).
43. Lu-Han-Lin, Wang Da-Hai, Xia Yi-Jun, Cui Yun-Feng and Chen Pao-Li, Physica Energieae Fortis Physica Nucl. 3 (1), 88 (1979).
44. K. Rusek, J. Turkiewicz, E. Zupranska and P. Zupranska, "Consolidated Progress Report for 1976 on Nuclear Data Activities in the NDS Service Area," INDC(SEC)-61/LN, International Atomic Energy Agency, Vienna, Austria, p. 229 (1977).
45. E. Zupranska, K. Rusek, J. Turkiewicz and P. Zupranska, Acta. Phys. Pol. B11, 853 (1980).
46. E. B. Paul and R. L. Clarke, Can. J. of Physics 31, 267 (1953).
47. J. F. Strain and W. J. Ross, "14-MeV Neutron Reactions," ORNL-3672, Oak Ridge National Laboratory, Oak Ridge, Tennessee (1965).
48. N. K. Majumdar and A. Chatterjee, Nucl. Phys. 41, 192 (1963).
49. D. J. Hughes and R. B. Schwartz, Brookhaven National Laboratory Report BNL-325 (2nd Edition) (1958); D. J. Hughes, B. A. Magurno, and M. K. Brussel, BNL-325 (2nd Edition, Suppl. 1) (1960).
50. V. N. Levkovskii, G. P. Vinit'skaya, G. E. Kovel'skaya and V. M. Stepanov, Sov. J. of Nucl. Phys. 10, 25 (1969).
51. A. Poularikas et al., A-ARK-60, 3, Univ. of Arkansas (1960). Data obtained from Computer Files on Microscopic Neutron Data, EXFOR 11683.003, International Atomic Energy Agency, Vienna.
52. I. Kumabe, J. Phys. Soc. Japan 13, 325 (1958).
53. Garuska et al., "Proc. of the 5th All Union Conf. on Neutron Physics," Kiev, USSR, 15-19 Sept. 1980.
54. H.H. Knitter, "A Review on Standard Fission Neutron Spectra of ²³⁵U and ²⁵²Cf," IAEA-208, International Atomic Energy Agency, Vienna, Austria, Vol. 1, p. 183 (1978).

55. W. P. Poenitz and T. Tamura, "Investigation of the Prompt-Neutron Spectrum for Spontaneously-Fissioning ^{252}Cf ," Nuclear Data for Science and Technology, Proceedings of an International Conference, Antwerp, Belgium, 6-10 September 1982, Ed. K. H. Boeckhoff, D. Reidel Publishing Company, Dordrecht, Netherlands, p. 465 (1983).
56. D. G. Madland and J. R. Nix, "Calculation of the Prompt Neutron Spectrum and Average Prompt Neutron Multiplicity for the Spontaneous Fission of ^{252}Cf ," *ibid.* Ref. 55, p. 473.
57. M. V. Blinov, G. S. Boykov and V. A. Vitenko, "New Experimental Data on the Energy Spectrum of ^{252}Cf Spontaneous Fission Prompt Neutrons," *ibid.* Ref. 55, p. 479.
58. R. Boettger, H. Klein, A. Chalupka and B. Strohmaier, "The Neutron Energy Spectrum from the Spontaneous Fission of ^{252}Cf in the Energy Range $2 \text{ MeV} \leq E_n \leq 14 \text{ MeV}$," *ibid.* Ref. 55, p. 484.
59. H. Maerten, D. Seeliger and B. Stobinski, "The High-energetic Part of the Neutron Spectrum from Spontaneous Fission of ^{252}Cf ," *ibid.* Ref. 55, p. 488.
60. J. Grundl and C. Eisenhauer, "Benchmark Neutron Fields for Reactor Dosimetry," *ibid.* Ref. 54, p. 53.
61. G. Winkler, D. L. Smith and J. W. Meadows, "On the Discrepancy Between Differential and Integral Results for the $^{63}\text{Cu}(n,\alpha)^{60}\text{Co}$ Cross Section," *ibid.* Ref. 8, p. 199.
62. Z. Deszo and J. Csikai, "Proc. of the 4th All Union Conf. on Neutron Physics," Kiev, USSR, 18-22 April 1977.
63. E. M. Gryntakis, *J. of Radioanalytical Chemistry* 52, 219 (1979).
64. N. D. Dudev and R. R. Heinrich, "Flux Characterization and Neutron Cross Section Studies in EBR-II," ANL-7629, Argonne National Laboratory (1970).
65. F. Nasyrov, *Soviet Atomic Energy* 25, 1251 (1968).
66. K. Kobayashi, I. Kimura, M. Nakazawa and M. Akiyama, *J. of Nucl. Sci. and Technology* 13, 531 (1976).
67. I. Kimura, K. Kobayashi and T. Shibata, *J. Nucl. Sci. and Technology* 8, 59 (1971).

68. Benjamin A. Magurno, "ENDF/B-V Data Testing Report, Contribution by the Special Application File Subcommittee (SAFE), Cross Section Evaluation Working Group (CSEWG)," unpublished report, National Nuclear Data Center, Brookhaven National Laboratory, Upton, New York 11973 (1982).
69. Katsuhei Kobayashi, Itsuro Kimura and Wolf Mannhart, *J. of Nucl. Sci. and Technology* 19, 341 (1982).
70. Donald L. Smith, "Analysis of the Sensitivity of Spectrum-Average Cross Sections to Individual Characteristics of Differential Excitation Functions," ANL/NDM-30, Argonne National Laboratory, Argonne, Illinois 60439 (1977).

TABLE 1. Calculated Neutron Multiple-Scattering Correction Parameters^a

E_n (MeV)	α	β	γ	ρ	<u>Net Correction η^b</u>
6.268	2.5	0.4	7.4	2.5	7.0
7.264	2.1	0.2	6.2	2.0	5.9
8.242	2.2	0.3	6.1	2.3	5.9
9.210	1.9	0.3	5.6	2.1	5.5
10.17	2.0	0.4	5.9	1.9	5.4

^a Parameters are defined in Ref. 26. All values are given in percent.

^b $\eta = |(\alpha + \beta) - (\gamma + \rho)|$.

TABLE 2: Sources of Experimental Error

RANDOM ERRORS

<u>Symbol</u>	<u>Magnitude (%)</u>	<u>Description</u>
R ₁	N ^a	Exposure, waiting and counting times.
R ₂	0.5 - 22.6	Gamma-ray yield.
R ₃	0.1 - 0.2	Fission yield.
R ₄	0.5	Extrapolation correction.
R ₅	1 - 3	Background-fission correction.
R ₆	N - 0.5 ^a	Background-activation correction.
R ₇	1.5	Geometric corrections.

SYSTEMATIC ERRORS

<u>Symbol</u>	<u>Magnitude (%)</u>	<u>Description</u>
S ₁	0.1 - 0.2	⁴⁸ Sc decay half life.
S ₂	2	²³⁸ U content of monitor deposit.
S ₃	0.2	⁵¹ V content of samples.
S ₄	0.8	Uranium-deposit thickness correction.
S ₅	1	Gamma-ray counting efficiency.
S ₆	N ^{a, b}	⁴⁸ Sc gamma-ray-decay branch factor.
S ₇	N ^{a, b}	Orientation of sample for counting.
S ₈	2	Neutron source properties.
S ₉	N ^a	Room-return fission events.

TABLE 2: Sources of Experimental Error (Continued)

RANDOM ERRORS

<u>Symbol</u>	<u>Magnitude (%)</u>	<u>Description</u>
S ₁₀	1.3 - 1.6	Neutron scattering corrections.
S ₁₁	1.5	Geometric corrections.
S ₁₂	2.6 - 12.2	Average neutron energy.

^a N = negligible

^b Uncertainty actually included in gamma-ray counting efficiency determination (S₅).

TABLE 3: Explicit Values for Variable Error Components^a

<u>Data Point</u>	<u>R₂</u>	<u>R₃</u>	<u>R₅</u>	<u>R₆</u>	<u>S₁</u>	<u>S₁₀</u>	<u>S₁₂</u>
1	22.6	0.2	1.0	N ^b	0.1	1.6	8.4
2	5.6	0.1	1.0	N	0.1	1.6	11.0
3	2.0	0.1	1.0	N	0.1	1.6	12.2
4	12.7	0.2	1.0	N	0.2	1.6	9.6
5	1.8	0.1	1.0	N	0.1	1.5	9.4
6	7.1	0.2	1.0	N	0.2	1.5	7.7
7	1.6	0.1	1.0	N	0.2	1.5	7.8
8	1.7	0.2	1.0	N	0.2	1.5	8.3
9	5.6	0.2	1.5	N	0.2	1.4	8.8
10	1.1	0.1	1.5	N	0.2	1.4	8.7
11	3.5	0.2	1.5	N	0.2	1.4	7.8
12	2.7	0.2	1.5	N	0.2	1.4	7.5
13	0.8	0.1	1.5	N	0.2	1.4	4.7
14	0.9	0.1	2.0	0.1	0.2	1.4	5.9
15	0.6	0.1	2.0	0.1	0.2	1.4	5.2
16	1.0	0.2	2.0	0.3	0.2	1.3	3.4
17	0.8	0.2	2.0	0.3	0.2	1.3	4.3
18	0.5	0.1	3.0	0.3	0.2	1.3	3.2
19	0.6	0.1	3.0	0.3	0.2	1.3	2.8
20	0.7	0.2	3.0	0.5	0.2	1.3	2.6

^a Values in percent. See Table 2 for error component descriptions.

^b N = Negligible

TABLE 4: Systematic-Error-Component Correlations

<u>Symbol</u>	<u>Assumed Correlations (%)</u>
S ₁	100
S ₂	100
S ₃	100
S ₄	100
S ₅	100
S ₆	Not applicable ^a
S ₇	Not applicable ^a
S ₈	(100-10 ΔE) ^b
S ₉	Not applicable ^a
S ₁₀	(100-10 ΔE) ^b
S ₁₁	100
S ₁₂	100

^a Error component is either negligible or uncertainty is included elsewhere, e.g., uncertainties normally associated with S₆ and S₇ are included in S₅.

^b ΔE is the magnitude of the difference in the neutron energies for the two data points, in MeV.

TABLE 5: $^{51}\text{V}(n, \alpha)^{48}\text{Sc}$ Reaction Cross-Section Results

Data Point	E_n (MeV)	Resolution ^a (MeV)	Measured Ratio	Ratio Random Error(%)	Ratio Systematic Error(%)	Ratio Total Error(%)	$\sigma_{F,238}^b$ (mb)	Error in $\sigma_{F,238}^b$	$\sigma_{n\alpha}$ (mb)	Error in $\sigma_{n\alpha}$ (%)
1	5.515	0.191	2.705(-6) ^c	22.7	9.2	24.5	549.4	2.6	0.001486	24.6
2	5.802	0.176	4.923(-6)	5.9	11.6	13.0	586.8	2.6	0.002889	13.3
3	6.073	0.166	1.203(-5)	2.7	12.8	13.1	639.5	3.9	0.007693	13.7
4	6.338	0.161	2.711(-5)	12.8	10.3	16.4	746.6	3.9	0.02024	16.9
5	6.338	0.158	2.826(-5)	2.6	10.1	10.4	746.6	3.9	0.02110	11.1
6	6.598	0.153	4.646(-5)	7.3	8.6	11.3	839.2	3.9	0.03899	11.9
7	6.598	0.154	5.230(-5)	2.5	8.7	9.1	839.2	3.9	0.04389	9.9
8	6.856	0.161	9.074(-5)	2.5	9.1	9.4	901.4	3.9	0.08179	10.2
9	7.110	0.170	1.677(-4)	6.0	9.6	11.3	936.2	3.9	0.1570	12.0
10	7.110	0.169	1.690(-4)	2.4	9.5	9.8	936.2	3.9	0.1582	10.5
11	7.363	0.173	2.809(-4)	4.1	8.6	9.5	969.2	3.9	0.2722	10.3
12	7.583	0.175	4.597(-4)	3.5	8.4	9.1	987.7	3.9	0.4540	9.9
13	7.862	0.184	7.849(-4)	2.3	6.0	6.4	989.9	3.9	0.7770	7.5
14	8.108	0.193	1.041(-3)	2.7	7.0	7.5	991.8	2.9	1.032	8.0
15	8.354	0.197	1.471(-3)	2.6	6.4	6.9	993.6	2.9	1.462	7.5
16	8.598	0.206	2.031(-3)	2.8	5.0	5.7	995.4	2.9	2.022	6.4
17	8.843	0.215	2.328(-3)	2.7	5.7	6.3	997.2	2.9	2.321	6.9
18	9.085	0.216	3.046(-3)	3.4	4.9	6.0	997.0	2.9	3.037	6.6
19	9.326	0.224	3.341(-3)	3.5	4.6	5.8	993.1	2.9	3.318	6.5
20	9.567	0.233	4.004(-3)	3.5	4.5	5.7	989.1	2.9	3.960	6.4

^a FWHM of incident-neutron distribution.

^b ^{238}U neutron-fission cross section, ENDF/B-V [3].

^c The notation 2.705(-6) signifies the value 2.705×10^{-6} .

TABLE 6: Error Correlation Matrix for the Present $51\text{V}(n,\alpha)^48\text{Sc-to-}^{238}\text{U}(n,f)$ Cross Section Ratiosa

Data Point	1	2	3	4	5	6	7	8	9	10	11	12	13	14	15	16	17	18	19	20
1	1	.34	.38	.24	.36	.28	.36	.36	.31	.36	.34	.34	.33	.34	.33	.29	.31	.27	.25	.24
2		1	.87	.56	.87	.67	.85	.86	.75	.86	.80	.81	.77	.80	.78	.67	.73	.61	.57	.54
3			1	.61	.95	.73	.92	.93	.82	.93	.87	.88	.84	.87	.84	.72	.79	.66	.61	.63
4				1	.65	.48	.60	.60	.53	.60	.57	.57	.55	.57	.55	.48	.52	.44	.41	.40
5					1	.74	.93	.93	.82	.93	.87	.88	.85	.88	.86	.75	.80	.68	.64	.61
6						1	.73	.73	.64	.73	.69	.69	.68	.89	.68	.60	.67	.55	.56	.50
7							1	.92	.80	.92	.86	.87	.86	.87	.86	.76	.81	.69	.65	.63
8								1	.81	.93	.87	.88	.86	.88	.86	.76	.81	.70	.65	.63
9									1	.82	.76	.77	.75	.77	.75	.66	.71	.61	.57	.55
10										1	.87	.89	.86	.88	.86	.79	.81	.69	.65	.63
11											1	.83	.82	.83	.82	.76	.80	.67	.63	.60
12												1	.84	.85	.83	.74	.82	.68	.64	.62
13													1	.86	.86	.80	.82	.78	.70	.68
14														1	.86	.78	.82	.72	.68	.66
15															1	.85	.89	.78	.75	.72
16																1	.78	.71	.69	.67
17																	1	.73	.70	.68
18																		1	.65	.64
19																			1	.63
20																				1

(symmetric)

aCalculated using information from Tables 2-4, according to methods described in Ref. 29.

TABLE 7: Experimental Fission-Spectrum-Average Cross Sections $\langle\sigma\rangle$ and Renormalized Values for $^{51}\text{V}(n,\alpha)^{48}\text{Sc}$

Origin	Date	Neutron Spectrum	Comparison Standard Reaction	Reported $\langle\sigma\rangle$ for Std. Reaction	Accepted $\langle\sigma\rangle$ for Std. Reaction	Reported $\langle\sigma\rangle$ for $^{51}\text{V}(n,\alpha)^{48}\text{Sc}$	Renormalized $\langle\sigma\rangle$ for $^{51}\text{V}(n,\alpha)^{48}\text{Sc}$
Kobayashi + (Ref. 66)	1976	Fast Reactor	$^{27}\text{Al}(n,\alpha)^{24}\text{Na}$	0.644 mb	0.720 mba	0.0197 ± 0.0012 mb	0.02202 ± 0.0013 mb
Kimura + (Ref. 67)	1971	Thermal Reactor (converter)	$^{27}\text{Al}(n,\alpha)^{24}\text{Na}$	0.63 mb	0.720 mba	0.0217 ± 0.0015 mb	0.02480 ± 0.0017 mb
Nasyrov (Ref. 65)	1968	Reactor (Unspecified)	$^{27}\text{Al}(n,\alpha)^{24}\text{Na}$	0.58 ± 0.07 mb	0.720 mba	0.0153 ± 0.0027 mb	0.01899 ± 0.0034 mb
Dudey + (Ref. 64)	1970	Fast Reactor	$^{63}\text{Cu}(n,\alpha)^{60}\text{Co}$	0.1 mb	0.507 mbb	0.0041 ($\pm 9.7\%$)	0.02079 ± 0.0034 mb
Deszo + (Ref. 62)	1977	^{252}Cf Source	$^{27}\text{Al}(n,\alpha)^{24}\text{Na}$	1.08 ± 0.05 mb	1.006 mba,c	0.043 ± 0.002 mb	0.0401 ± 0.0019 mb

aRef. 68.

bRef. 61.

cRef. 69.

TABLE 8. Representation of $\sigma(E)$ for $^{51}\text{V}(n,\alpha)^{48}\text{Sc}$ Based on Consideration of the Present Experimental Data and Two Previous Evaluations^a

<u>E</u> (MeV)	<u>$\sigma(E)$</u> (mb)	<u>E</u> (MeV)	<u>$\sigma(E)$</u> (mb)
4.0	9.408(-5) ^b	7.8	0.7190
4.2	1.584(-4)	7.9	0.8180
4.4	2.112(-4)	8.0	0.9150
4.6	2.606(-4)	8.1	1.040
4.8	3.486(-4)	8.2	1.200
5.0	4.960(-4)	8.3	1.410
5.2	7.515(-4)	8.4	1.610
5.4	1.143(-3)	8.5	1.800
5.6	1.813(-3)	8.6	1.960
5.8	3.043(-3)	8.7	2.120
5.9	4.150(-3)	8.8	2.300
6.0	6.030(-3)	8.9	2.540
6.1	9.050(-3)	9.0	2.790
6.2	1.350(-2)	9.1	3.010
6.3	1.850(-2) ²	9.2	3.170
6.4	2.470(-2)	9.3	3.330
6.5	3.200(-2)	9.4	3.540
6.6	4.140(-2)	10.0	4.840
6.7	5.410(-2)	10.5	5.496
6.8	7.000(-2)	11.0	6.0
6.9	9.100(-2)	12.0	9.0
7.0	0.1175	13.0	12.0
7.1	0.1530	14.0	15.0
7.2	0.1935	15.0	17.5
7.3	0.2470	16.0	19.5
7.4	0.3120	17.0	20.0
7.5	0.4000	17.5	20.5
7.6	0.5040	18.0	20.0
7.7	0.6140	19.0	18.0
		20.0	15.0

^a See Section V of text for the origin of this representation. In the present work, values of $\sigma(E)$ at energies other than grid points are deduced by linear interpolation.

^b The notation 9.408(-5) signifies the value 9.408×10^{-5} .

TABLE 9. Summary of Present Fission-Spectrum-Average Cross Section Calculations for $^{51}\text{V}(n,\alpha)^{48}\text{Sc}$

Calculated $\langle\sigma\rangle$ Values^a

Origin of $\sigma(E)$	$\phi(E)$	
	^{235}U Spectrum ^b	^{252}Cf Spectrum ^c
ENDF/B/V ^b	0.02228 mb	0.03710 mb
JENDL-2 ^d	0.02798 mb	0.04370 mb
Present Work ^e	0.02377 mb	0.03887 mb

Response Contributions^f

Neutron Energy Range (MeV)	$\phi(E)$	
	^{235}U Spectrum ^b	^{252}Cf Spectrum ^c
< 5.5	0.3%	0.2%
5.5 - 9.6	51.1%	44.9%
> 9.6	48.6%	54.9%

^a Eq. (1) from text.

^b Ref. 3.

^c Refs. 55 and 56.

^d Ref. 4.

^e Table 8.

^f Contributions to $\langle\sigma\rangle$ (as calculated using Eq. (1) from text) from various energy regions are indicated for $\sigma(E)$ given in Table 8.

FIGURE CAPTIONS

Symbol List (Figs. 1-5):

○ Present work	■ Borman + (Ref. 38)	E Paul + (Ref. 46)
□ Crumpton (Ref. 31)	⊗ Hillman (Ref. 39)	S Strain + (Ref. 47)
⊗ Paulsen + (Ref. 32)	⊗ Vonach (Ref. 40)	M Majumder + (Ref. 48)
⊗ Warren + (Ref. 33)	⊗ Mannhart + (Ref. 41)	H Hughes + (Ref. 49)
△ Robertson + (Ref. 34)	⊗ Vonach + (Ref. 42)	L Levkovskii + (Ref. 50)
⊗ Bramlitt + (Ref. 35)	⊗ Lu-Han-Lin + (Ref. 43)	P Poularikas + (Ref. 51)
⊗ Qaim (Ref. 36)	⊗ Rusek + (Ref. 44)	K Kumabe + (Ref. 52)
⊗ Schwerer + (Ref. 37)	● Zupranska + (Ref. 45)	G Garuska + (Ref. 53)

- Fig. 1. Cross sections for the $^{51}\text{V}(n,\alpha)^{48}\text{Sc}$ reaction. Data points are identified above. Curve is the ENDF/B-V evaluation [3]. Values above 10 MeV can be seen more clearly in Fig. 4.
- Fig. 2. Present experimental $^{51}\text{V}(n,\alpha)^{48}\text{Sc}$ cross sections in the energy range 7-10 MeV. Curve is the ENDF/B-V evaluation [3].
- Fig. 3. Cross sections for the $^{51}\text{V}(n,\alpha)^{48}\text{Sc}$ reaction. Data points are identified above. Curves are: A- ENDF/B-V evaluation [3], B - JENDL-2 evaluation [4]. Values above 10 MeV can be seen more clearly in Fig. 4.
- Fig. 4. Experimental $^{51}\text{V}(n,\alpha)^{48}\text{Sc}$ cross sections above 10 MeV from the literature [1, 31-53]. Data points are identified above. Curves are: A- ENDF/B-V evaluation [3], B- JENDL-2 evaluation [4].
- Fig. 5. Cross sections for the $^{51}\text{V}(n,\alpha)^{48}\text{Sc}$ reaction. Data points are identified above. Curve corresponds to Table 8, and it is based on an eyeguide to the present data and portions of two previous evaluations (see Section V of text). This curve is used to calculate spectrum-average cross sections.
- Fig. 6. ^{235}U fission spectrum response analysis for $^{51}\text{V}(n,\alpha)^{48}\text{Sc}$. The cross section is based on the present work (Fig. 5 and Table 8). The neutron spectrum is the standard ^{235}U thermal-neutron-induced-fission neutron spectrum from ENDF/B-V [3]. Shown are separate plots of SIG - $\sigma(E)$, PHI - $\phi(E)$, SIG*PHI - $\sigma(E)\phi(E)$, and SIGP*PHI - $\partial\sigma/\partial E(E)\phi(E)$, all versus energy E from 0 to 20 MeV. Each plot has its own individual relative ordinate scale. The plot of SIG*PHI indicates the response energy range while that for SIGP*PHI shows the region of greatest energy scale sensitivity for the reaction.

- Fig. 7. ^{252}Cf fission spectrum response analysis for $^{51}\text{V}(n,\alpha)^{48}\text{Sc}$. The cross section is based on the present work (Fig. 5 and Table 8). The neutron spectrum is the standard ^{252}Cf spontaneous-fission neutron spectrum (e.g., Refs. 55 and 56). Shown are plots of $\text{SIG} \cdot \sigma(E)$, $\text{PHI} \cdot \phi(E)$, $\text{SIG} \cdot \text{PHI} = \sigma(E)\phi(E)$, and $\text{SIGP} \cdot \text{PHI} = \partial\sigma/\partial E(E)\phi(E)$, all versus energy E from 0 to 20 MeV. Each plot has its own individual relative ordinate scale. The plot of $\text{SIG} \cdot \text{PHI}$ indicates the response energy range while that for $\text{SIGP} \cdot \text{PHI}$ shows the region of greatest energy scale sensitivity for the reaction.
- Fig. 8. Comparison of experimental and calculated ^{235}U fission-spectrum integral results. Data points: Ref. 66 (●), Ref. 67 (X), Ref. 65 (○), Ref. 64 (■). These are renormalized experimental values (see Section V of text). Calculated values: ENDF/B-V [3] (E), JENDL-2 [4] (J), and present work - Table 8 (vertical line plus dashed lines showing $\pm 7\%$ uncertainty). Calculations utilize Eq. (1) from the text. Spectrum is from ENDF/B-V[3].
- Fig. 9. Comparison of experimental and calculated ^{252}Cf fission-spectrum integral results. Data point: Ref. 62 (●). This value is renormalized (see Section V of text). Calculated values: ENDF/B-V [3], JENDL-2 [4] (J), and present work - Table 8 (vertical line plus dashed lines showing $\pm 7\%$ uncertainty). Calculations utilize Eq. (1) from the text. Spectrum is based on Refs. 55 and 56.

Figure 1

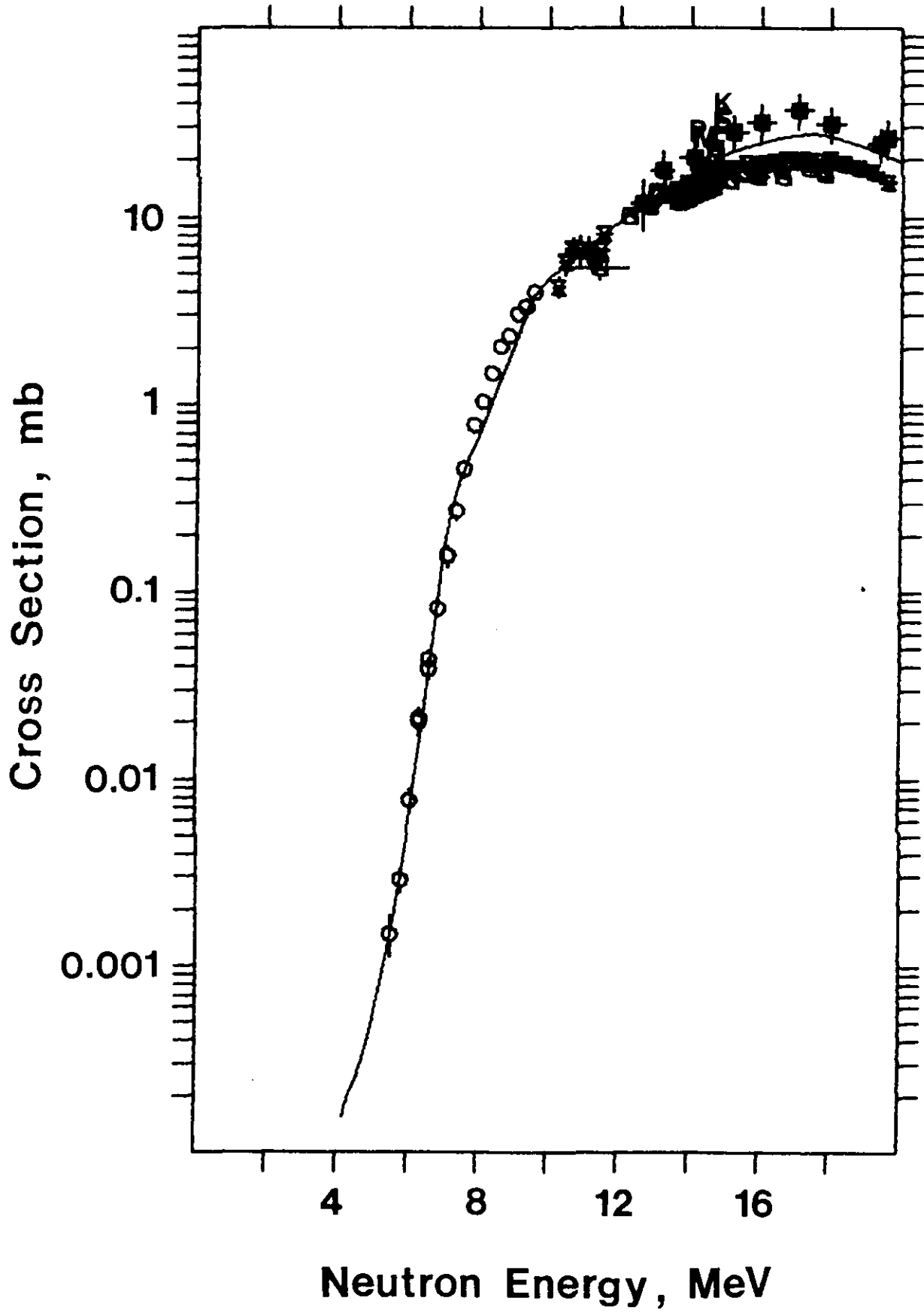


Figure 2

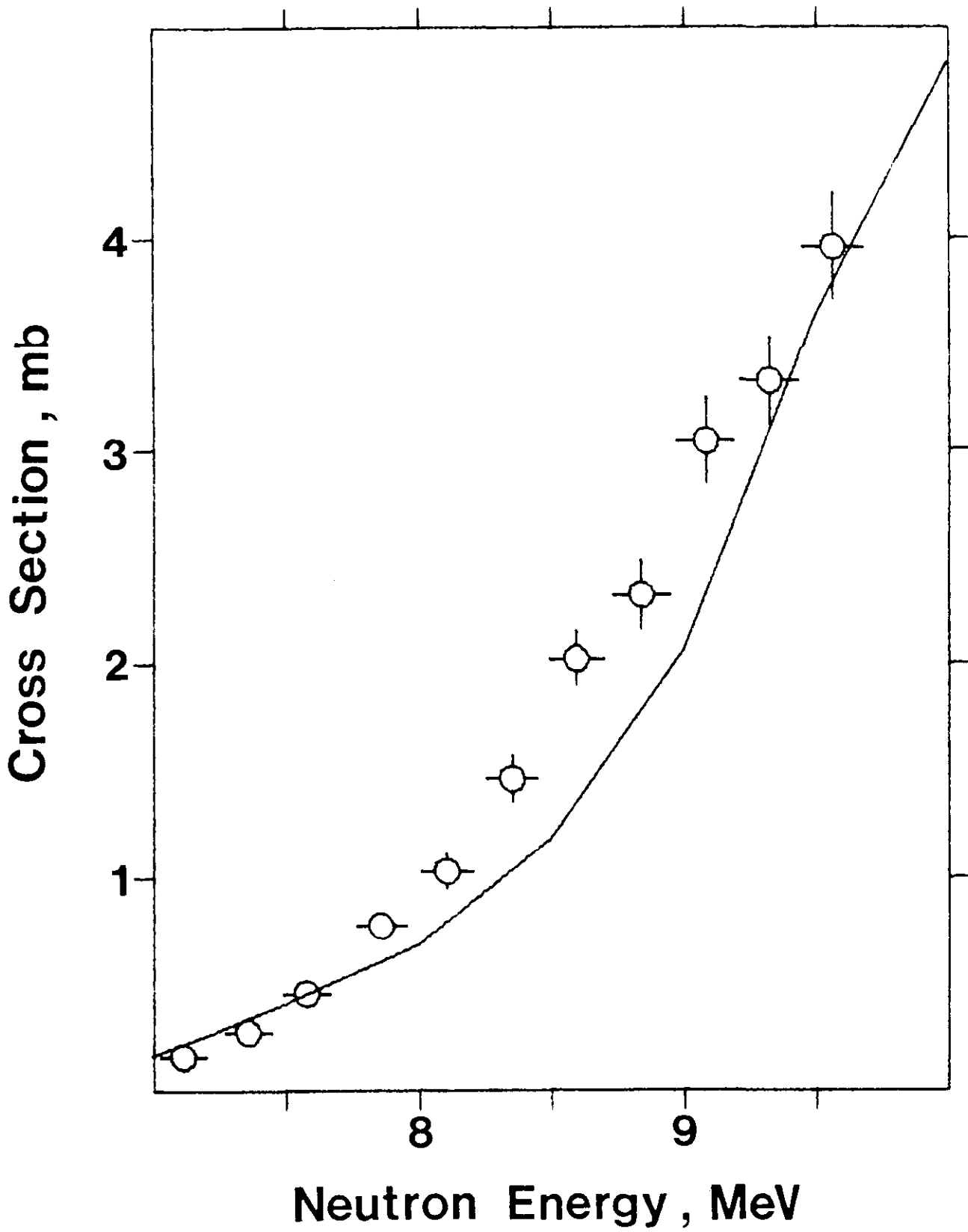


Figure 3

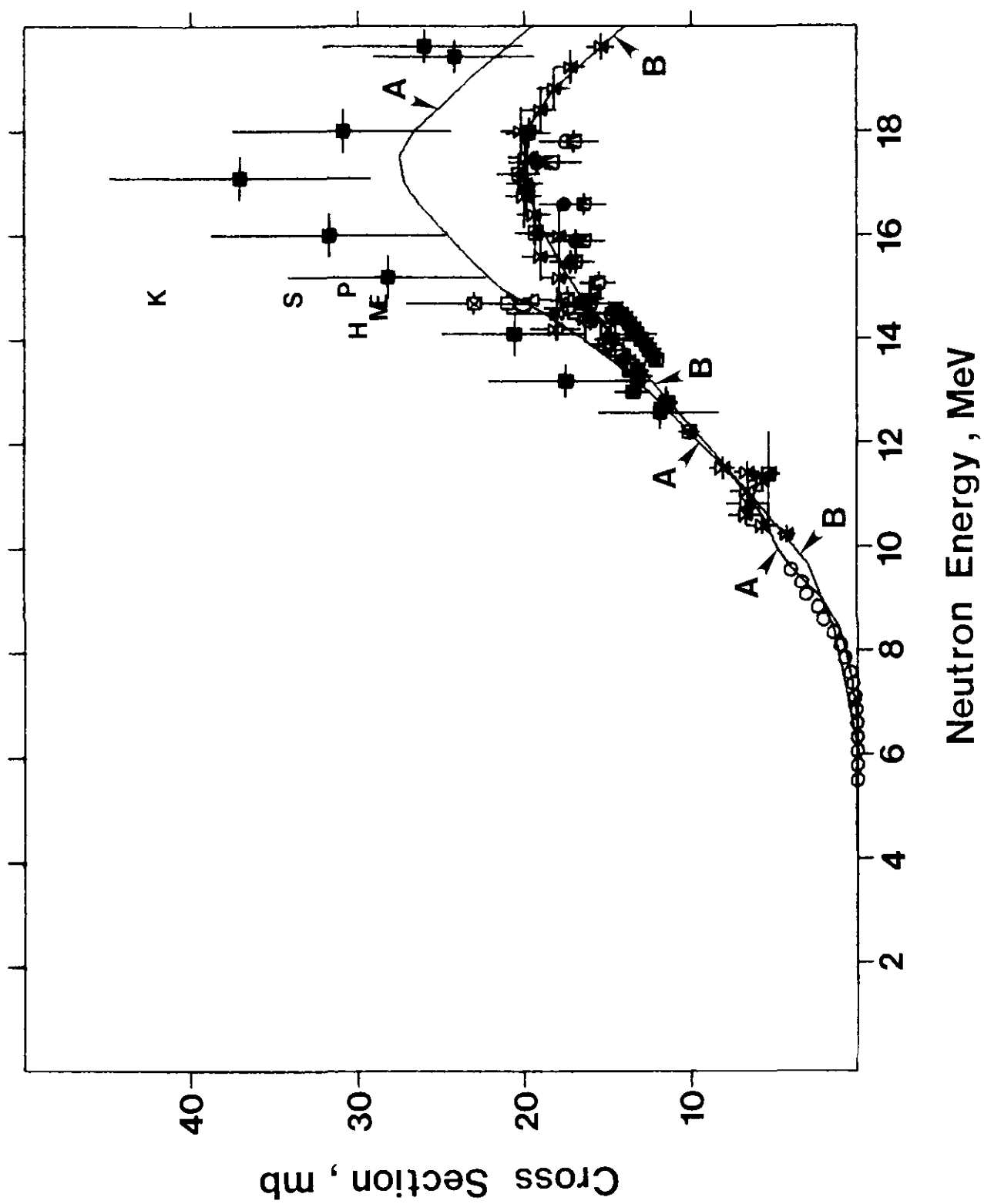


Figure 4

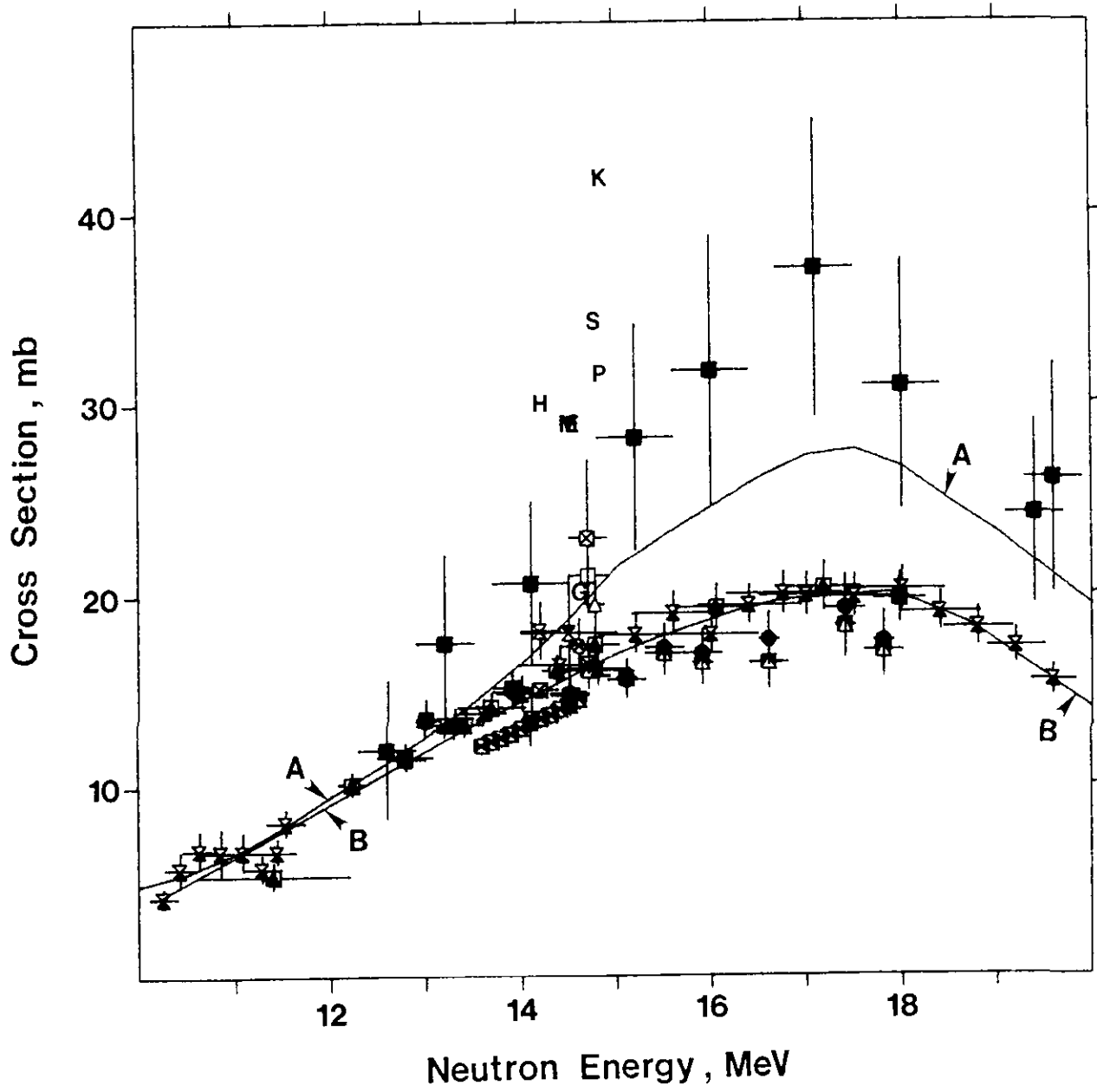
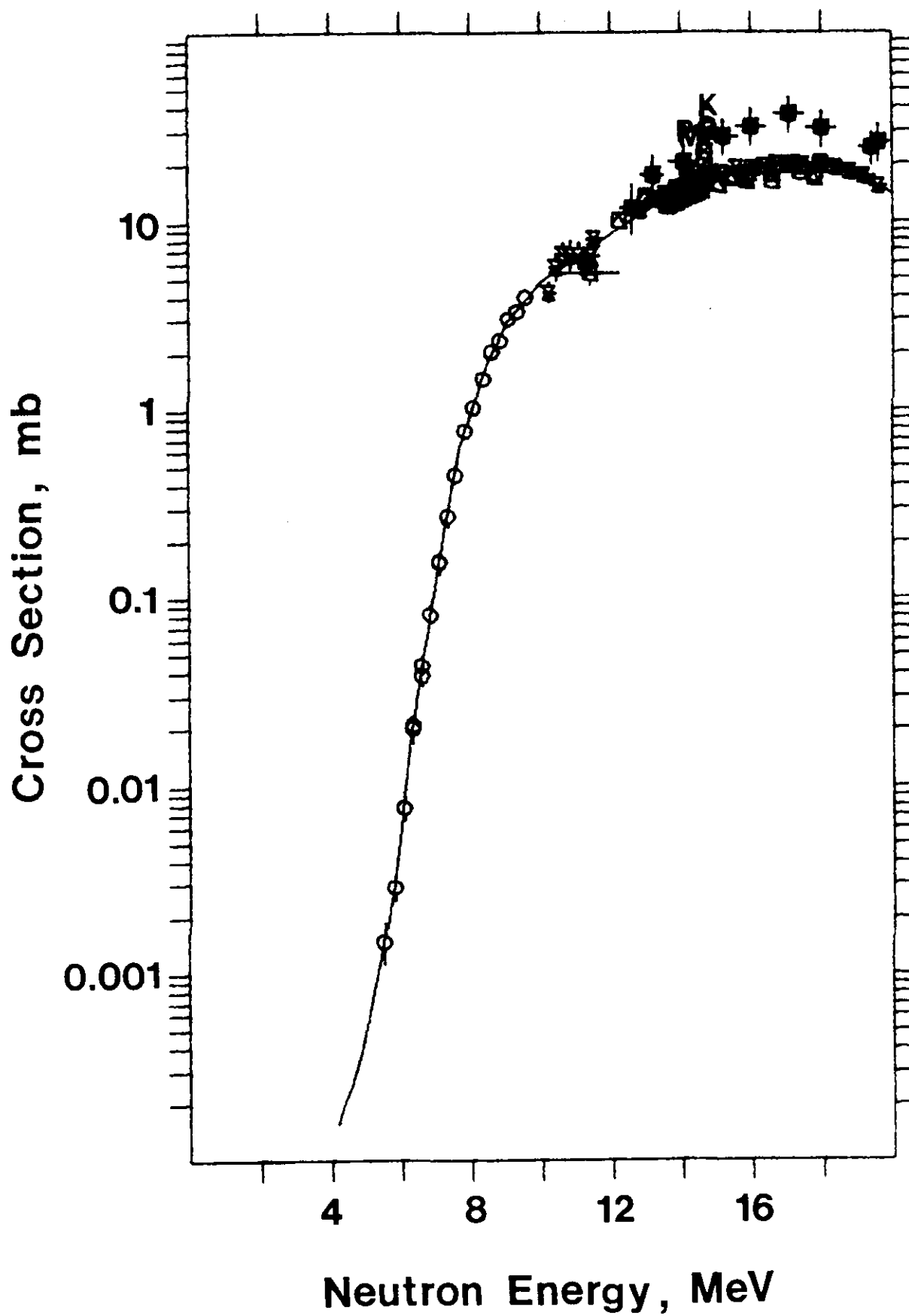
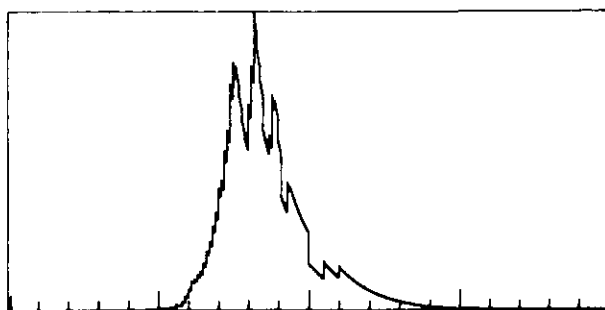
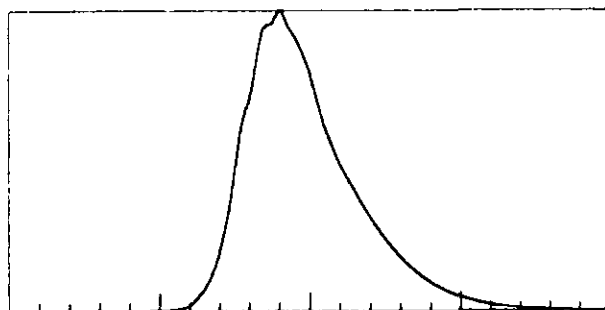


Figure 5

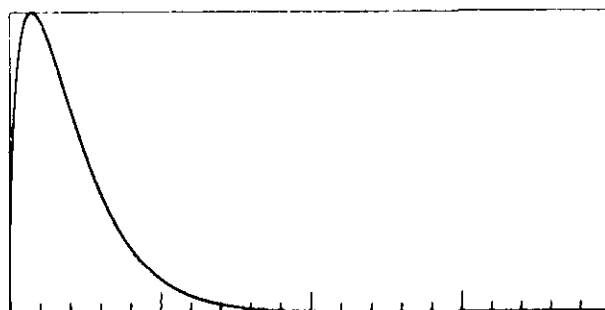




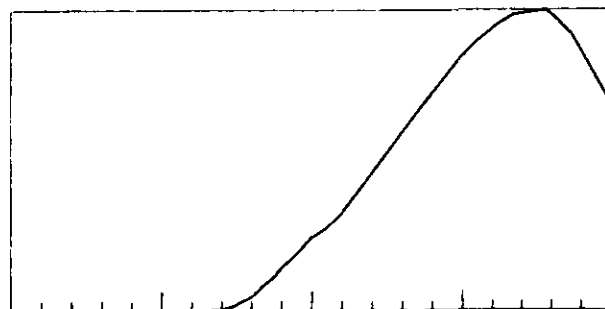
SIG*PHI



SIG*PHI



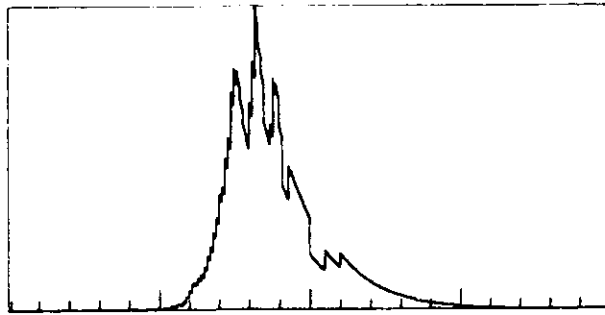
PHI



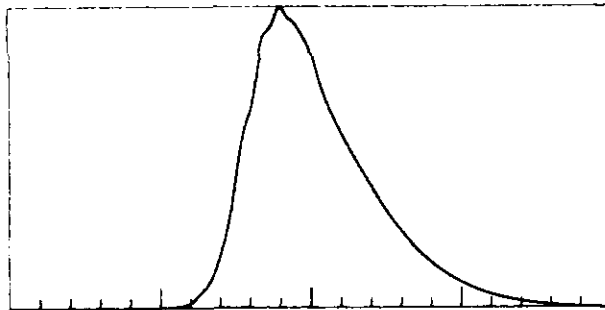
SIG

TH U5 FISSION WATTS V

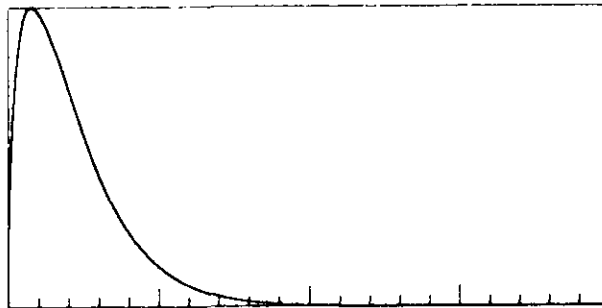
V-51(N,ALFA)SC-48 PRESENT WORK



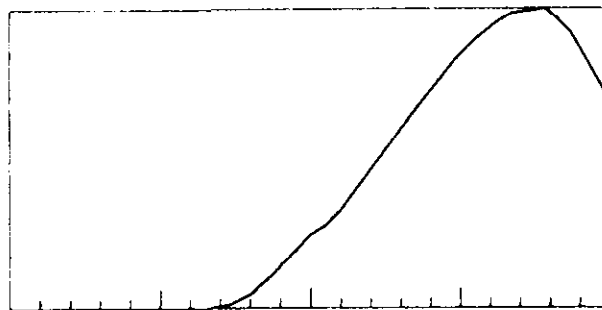
SIGP*PHI



SIG*PHI



PHI



SIG

CF BASED ON WPP AND LANL
V-51(N,ALFA)SC-48 PRESENT WORK

Figure 8

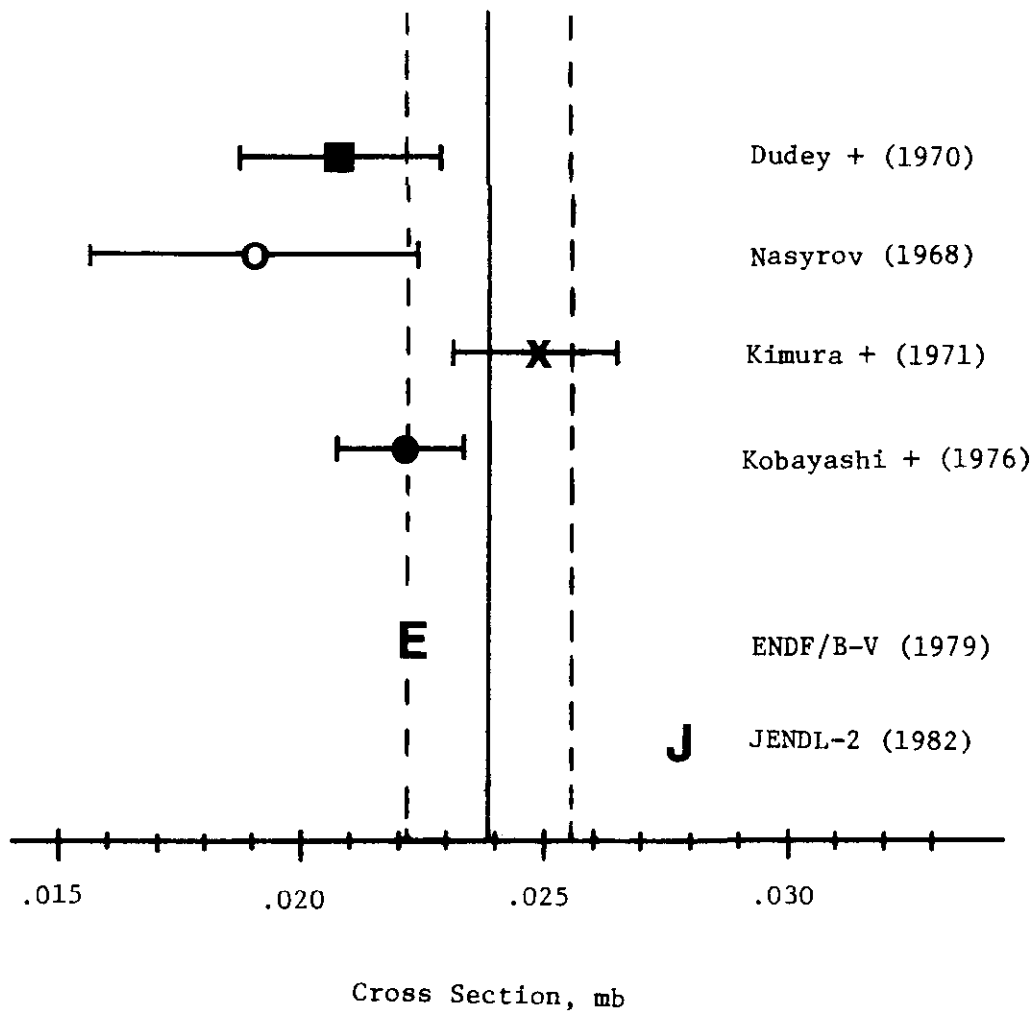


Figure 9

